was warmed to room temperature and then was stirred for 2 h 45 min. Then a saturated aqueous solution of NH_4Cl was added until a clear organic layer resulted. Subsequent drying ($MgSO_4$) and removal of solvent at reduced pressure was followed by GLC analysis of the residue and then fractional distillation of the product, **7**, bp 48–50 °C (0.1 mmHg).

Reaction of 3 with Benzaldehyde/Me_3SiCl (Example of Procedure A). A solution of **3** in 40 mL of hexane was prepared by reaction of 4.610 g (0.0319 mol) of **2**, 7.6 mL (0.0504 mol) of TMEDA, and 25 mL of 1.7 M *t*-BuLi (0.0425 mol) in pentane. With use of procedure A (above), 4.4 mL (0.0433 mol) of benzaldehyde was added by syringe over a period of 5 min. After the mixture had been stirred for 15 min at room temperature, 5.8 mL (0.046 mol) of Me_3SiCl was added dropwise by syringe. After 20 min the mixture was filtered through Celite. Removal of solvents from the filtrate at reduced pressure (room temperature, 60 mmHg) was followed by GLC analysis of the residue and then fractional distillation of the product, **14**, at 82.5–84 °C (0.07 mmHg).

Reaction of 3 with Benzoyl Chloride (Procedure B). A solution of **3** in 20 mL of hexane was prepared by the reaction of 3.929 g (0.0214 mol) of **2**, 6.2 mL (0.0411 mol) of TMEDA, and 20.8 mL of 1.7 M *t*-BuLi (0.0354 mol) in pentane. It then was added to a solution of 5.00 g (0.0356 mol) of benzoyl chloride in 30 mL of Et_2O at −40 °C over a period of 10 min. After the mixture had been stirred at −40 °C for 45 min, it was warmed to room temperature and stirred for 14 h. Standard workup with saturated aqueous NH_4Cl followed. Subsequent drying ($MgSO_4$) and removal of solvent at reduced pressure was followed by GLC analysis of the residue and then fractional distillation of the product, **15**, bp 70 °C (0.05 mmHg).

Reaction of 3 with Benzonitrile (Procedure B). The same general procedure as described in the experiment above was used in the reaction of **3** (from 0.0266 mol of **2**) and 0.0353 mol of benzonitrile at −78 °C and then at room temperature. Subsequently, 1.1 mL of MeOH was added dropwise. Filtration through Celite was followed by solvent removal at reduced pressure and then fractional distillation of the product, **16**, at 70–71 °C (0.05 mmHg).

Acknowledgment. We are grateful to the U.S. Air Force Office of Scientific Research (AFSC) for generous support of this research.

Registry No. **2**, 1627-98-1; **3**, 129152-58-5; **4**, 129152-59-6; **5**, 129152-60-9; **6**, 129152-61-0; **7**, 129152-62-1; **8**, 129152-63-2; **9**, 129152-64-3; **10**, 129152-65-4; **11**, 129152-66-5; **12**, 129152-67-6; **13**, 129152-68-7; **14**, 129152-69-8; **15**, 129152-70-1; **16**, 129152-71-2; Me_3SiCl, 75-77-4; Me_2HSiCl, 1066-35-9; $CH_3CH_2CH_2I$, 107-08-4; Me_3SnCl, 1066-45-1; ICH_2CH_2I, 624-73-7; $BrCH_2CH_2Br$, 106-93-4; MeSSMe, 624-92-0; MeC(O)H, 75-07-0; PhC(O)H, 100-52-7; PhC(O)Cl, 98-88-4; PhCN, 100-47-0.

Facile Conversion of Organometallic Halide Complexes to Halomethyl Derivatives: Synthesis, Structure, and Reactivity of the $(\eta^5\text{-}C_5R_5)Cr(NO)_2CH_2X$ Series (R = H, CH_3; X = Cl, Br, I, OCH_3, OCH_2CH_3, PPh_3, CN, $SO_3C_6H_4CH_3$)

John L. Hubbard*,[1a] and William K. McVicar[1b]

Department of Chemistry and Biochemistry, Utah State University, Logan, Utah 84322-0300, and Department of Chemistry, University of Vermont, Burlington, Vermont 05405

Received February 6, 1990

Treatment of $(\eta^5\text{-}C_5R_5)Cr(NO)_2X$ with ethereal diazomethane in the presence of Cu powder provides access to the new $(\eta^5\text{-}C_5R_5)Cr(NO)_2CH_2X$ derivatives in 88–93% yield (R = H, CH_3; X = Cl, Br). In contrast to the chemistry of the isoelectronic/isostructural $(\eta^5\text{-}C_5H_5)Fe(CO)_2CH_2X$ systems, the CH_2 of the halomethyl ligand in the $(\eta^5\text{-}C_5H_5)Cr(NO)_2CH_2Cl$ complex undergoes a remarkably facile migration into a C–H bond of the coordinated $\eta^5\text{-}C_5H_5$ ring upon abstraction of the α-halide, giving the $(\eta^5\text{-}C_5H_4Me)Cr(NO)_2^+$ cation in >80% yield. Deuterium labeling shows the process to be *intramolecular*. Methylene migration is attributed to the extremely electrophilic nature of the Cr–alkylidene species generated upon halide abstraction. Intermolecular CH_2 transfer is only observed when $\eta^5\text{-}C_5Me_5$ derivatives are treated with Ag^+ in the presence of excess cyclohexene. The stable iodomethyl derivatives are obtained in high yield by simple NaI/THF metathesis from the chloromethyl complexes. The $(\eta^5\text{-}C_5Me_5)Cr(NO)_2CH_2I$ complex has been characterized by single-crystal X-ray diffraction methods: monoclinic space group $P2_1/a$, a = 10.366 (3) Å, b = 10.974 (2) Å, c = 12.818 (3) Å, β = 90.81 (2)°, Z = 4, final R/R_w = 7.47%/6.86%. The iodomethyl carbon–Cr distance of 2.093 (11) Å can be considered short for a Cr^0–C single bond. The halomethyl halide is irreversibly displaced by Y^- (Y^- = cyanide, tosylate, and alkoxides) to give stable $(\eta^5\text{-}C_5R_5)Cr(NO)_2CH_2Y$ derivatives. Reaction of $(\eta^5\text{-}C_5H_5)Cr(NO)_2CH_2I$ with PPh_3 followed by $NaBPh_4$ gives the cationic ylide $(\eta^5\text{-}C_5H_5)Cr(NO)_2CH_2PPh_3^+BPh_4^-$, which has been characterized by X-ray crystallography: monoclinic space group $P2_1/c$, a = 10.038 (2) Å, b = 23.587 (4) Å, c = 17.150 (3) Å, β = 102.35 (1)°, Z = 4, final R/R_w = 4.81%/5.42%. A C–P bond distance of 1.748 (3) Å indicates considerable ylide character for the CH_2PPh_3 ligand; the IR and NMR data show the CH_2PPh_3 ligand to be a stronger donor than the CH_2I ligand. The Cr–C distance for the CH_2PPh_3 ligand is 2.115 (3) Å in this case.

Introduction

α-substituted alkyl ligands (CH_2X) coordinated to transition metals continue to attract attention with regard to fundamental metal–carbon interactions. Hydroxymethyl and alkoxymethyl complexes are closely tied to the chemistry of vitamin B_{12},[2] the reduction of carbon monoxide in catalytic schemes such as the Fischer–Tropsch process,[3] and hydroformylation reactions.[4] Halomethyl

(1) (a) Utah State University. (b) University of Vermont.

(2) (a) Schrauzer, G. N.; Windgasser, R. J. *J. Am. Chem. Soc.* **1967**, *89*, 1999. (b) Hammer, R.; Klein, H. F. *Z. Naturforsch., A* **1977**, *32A*, 138. (c) Beck, W.; Kemmerich, T.; Boehme, H. *Z. Naturforsch., B* **1979**, *34B*, 200. (d) McBride, B. C.; Wolfe, R. S. *Nature* **1971**, *234*, 551.

0276-7333/90/2309-2683$02.50/0

complexes have received attention since they can often be converted to hydroxymethyl or alkoxymethyl complexes.[5] Halomethyl and alkoxymethyl complexes have been frequently used as metal–alkylidene precursors in cyclopropanation reactions.[6] Transient electrophilic methylidene complexes generated from halomethyl precursors have been utilized as alkylating agents toward coordinated vinyl, allyl, and acetyl ligands.[7] Other work has focused on using halomethyl or alkoxymethyl complexes together with organometallic nucleophiles, such as $(\eta^5\text{-}C_5H_5)M(CO)_2^-$, to give bridging methylene complexes (M = Fe, Ru).[8] Roper has shown the close relationship of methylidene halide complexes to halomethyl complexes.[9] The chemistry of Cr(III)–halomethyl coordination complexes has also been an active area of research.[10]

In contrast to the availability of main-group-metal–halomethyl compounds from the direct reaction of diazomethane with metal halide precursors,[11] there are fewer examples of transition-metal halides being converted directly to halomethyl derivatives by reaction with diazomethane.[12] There are a few reports of other diazoalkanes reacting with metal halide complexes to give halo alkyl complexes.[13] Piper and Wilkinson's reported conversion of $(\eta^5\text{-}C_5H_5)Cr(NO)_2Cl$ to $(\eta^5\text{-}C_5H_5)Cr(NO)_2CH_2Cl$ is the earliest report utilizing the copper-catalyzed decomposition of diazomethane.[14] Unfortunately, the low yield of this reaction and the lack of alternative synthetic routes has prevented the complete characterization of this family of halomethyl complexes.

Our present report begins with a reinvestigation of the reaction reported by Piper and Wilkinson.[14] Herein, we show that optimization of the reaction conditions makes the synthesis and derivatization of new metal dinitrosyl halomethyl complexes a straightforward process. Halide abstraction from these new complexes results in a surprising mode of reactivity, in which the methylene moiety migrates into a C–H bond of the $\eta^5\text{-}C_5H_5$ ligand.[15] In addition, we show that the halomethyl complexes can be readily converted to a variety of derivatives by nucleophilic halide displacement. When possible, we compare the properties of the new $(\eta^5\text{-}C_5R_5)Cr(NO)_2CH_2X$ complexes to those reported for the isoelectronic $(\eta^5\text{-}C_5R_5)Fe(CO)_2CH_2X$ complexes.

Results and Discussion

Synthesis and Characterization of the $(\eta^5\text{-}C_5R_5)Cr(NO)_2CH_2X$ Complexes. When the reaction between $(\eta^5\text{-}C_5H_5)Cr(NO)_2Cl$ (**1a**) and CH_2N_2 in Et_2O is carried out as described in the literature,[14] IR spectroscopy reveals that the CH_2N_2 is almost completely consumed after 10 min with no detectable product formation. However, the *slow* addition of ethereal CH_2N_2 to a Et_2O slurry of **1a** and Cu powder over a period of 30 min gives $(\eta^5\text{-}C_5H_5)Cr(NO)_2CH_2Cl$ (**2a**) in 88% yield after chromatography and recrystallization (eq 1). No reaction occurs in the absence

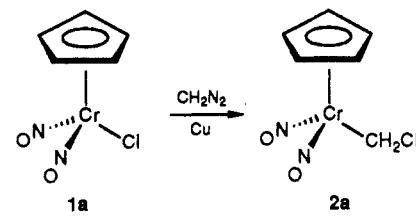

1a **2a** (1)

of Cu powder. Simply stirring the starting halide with Cu powder also results in no detectable reaction. The reaction is unaffected by changing the solvent to THF or CH_2Cl_2. The reaction does become sluggish when run in benzene, giving only 20–30% conversion of **1a** to **2a** compared to reactions run in Et_2O in the same time frame. Attempts to scale up the reaction indicate that Cu "poisoning" (due to a buildup of polymethylene) can slow the conversion rate: in reactions where addition of CH_2N_2 is required over periods longer than 30 min, the addition of fresh Cu powder is necessary in order to force the reaction to completion. Decreased gas evolution and the persistence of CH_2N_2 in the IR spectra after 30 min show that diazomethane decomposition is greatly slowed as the hydrocarbon residue accumulates. Blank reactions between ethereal diazomethane and Cu powder in CH_2Cl_2 over a 15-min period result in gas evolution, leaving a white, waxy hydrocarbon residue after solvent removal. This waxy residue has ^1H NMR resonances at δ 0.88 and 1.22 as well as several absorptions between δ 3.3 and 4.4. A similar product, lacking the ^1H NMR resonances in the δ 3.3–4.4 region, is obtained when the CH_2Cl_2 solvent is replaced by Et_2O or THF. The properties of the residue are consistent with oligomeric polymethylene. The signals between δ 3.3 and 4.4 seen in the case where CH_2Cl_2 is used as solvent are possibly due to CH_2Cl end groups resulting from polymer termination by solvent-generated CH_2Cl groups.

The active species responsible for converting the metal halides to metal–halomethyl products is apparently a transient produced from the Cu-catalyzed decomposition of CH_2N_2 and not CH_2N_2 itself. Recent matrix isolation work has shown the existence of $Cu{=}CH_2$ species formed upon the reaction of CH_2N_2 with Cu atoms.[16a] The de-

(3) (a) Heterogeneous review: Henrici-Olive, G.; Olive, S. *J. Mol. Catal.* **1984**, *24*, 247. (b) Maitlis, P. M.; Saez, I. M.; Meanwell, N. J.; Isobe, K.; Nutton, A.; Vaquez de Miguel, A.; Brucs, D. W.; Okeya, S.; Bailey, P. M.; Andrews, D. G.; Ashton, P. R.; Johnstone, J. R. *Nouv. J. Chim.* **1989**, *13*, 419. (c) Maitlis, P. M. *Pure Appl. Chem.* **1989**, *61*, 1747.

(4) (a) Pruett, R. *Adv. Organomet. Chem.* **1979**, *17*, 1. (b) Chan, A. S. C.; Carroll, W. E.; Willis, D. E. *J. Mol. Catal.* **1983**, *19*, 377. (c) Marko, L. *J. Organomet. Chem.* **1988**, *357*, 481.

(5) (a) Moss, J. R.; Pelling, S. *J. Organomet. Chem.* **1982**, *236*, 221. (b) Lapinte, C.; Astruc, D. *J. Chem. Soc., Dalton Trans.* **1983**, 430. (c) Thorn, D. L. *Organometallics* **1986**, *5*, 1897. (d) Nelson, G. O. *Organometallics* **1983**, *2*, 1474.

(6) For a recent review of this area see: Brookhart, M.; Studabaker, W. B. *Chem. Rev.* **1987**, *87*, 411.

(7) Cutler, A. R.; Bodnar, T. W. *Organometallics* **1985**, *2*, 1558.

(8) (a) Casey, C. P.; Fagan, P. J.; Miles, W. H. *J. Am. Chem. Soc.* **1982**, *104*, 1134. (b) Pettit, R.; Kao, S. C.; Thiel, C. H. *Organometallics* **1983**, *2*, 914. (c) Wright, M. E.; Nelson, G. O. *J. Organomet. Chem.* **1984**, *263*, 371. (d) Lin, Y. C.; Calabrese, J. C.; Wreford, S. S. *J. Am. Chem. Soc.* **1983**, *105*, 1679.

(9) (a) Roper, W. R.; Hoskins, S. V.; Rickard, C. E. F. *J. Chem. Soc., Chem. Commun.* **1984**, 1000. (b) Roper, W. R.; Clark, G. R.; Wright, A. H. *J. Organomet. Chem.* **1984**, *273*, C17.

(10) (a) Anet, F. A. L. *Can. J. Chem.* **1959**, *37*, 58. (b) Dodd, D.; Johnson, M. D. *J. Chem. Soc. A* **1968**, 34. (c) Bushey, W. R.; Espenson, J. H. *Inorg. Chem.* **1977**, *16*, 2772. (d) Azran, J.; Cohen, H.; Meyerstein, D. J. *J. Coord. Chem.* **1977**, *6*, 249. (e) Bakac, A.; Espenson, J. H.; Miller, L. P. *Inorg. Chem.* **1982**, *21*, 1557. (f) Nohr, R. S.; Spreer, L. O. *Inorg. Chem.* **1974**, *13*, 1239. (g) Byington, J. I.; Peters, R. D.; Spreer, L. O. *Inorg. Chem.* **1979**, *18*, 3324 and references therein. (h) Ogino, H.; Shoji, M.; Abe, Y.; Shimura, M.; Shimoi, M. *Inorg. Chem.* **1987**, *26*, 2542.

(11) (a) Seyferth, D. *Chem. Rev.* **1955**, *55*, 1155. (b) Lappert, M. F.; Poland, J. S. *Adv. Organomet. Chem.* **1970**, *9*, 397.

(12) (a) Mango, F. D.; Dvoretzky, I. *J. Am. Chem. Soc.* **1966**, *88*, 1654. (b) Herrmann, W. A. *Angew. Chem., Int. Ed. Engl.* **1978**, *17*, 800. (c) McCrindle, R.; Arsenault, G. J.; Ferguson, G.; McAlees, A. J.; Rahl, B. L.; Sneddon, D. W. *Organometallics* **1986**, *5*, 1171. (d) McCrindle, R.; Asenault, G. J.; Farwah, R. *J. Chem. Soc., Chem. Commun.* **1986**, 943. (e) McCrindle, R.; Sneedon, D. W. *J. Organomet. Chem.* **1985**, *282*, 413. (f) McCrindle, R.; Arsenault, G. J.; Farwaha, R. *J. Organomet. Chem.* **1985**, *296*, C51.

(13) (a) Reimer, K. J.; Shaver, A. *Inorg. Chem.* **1975**, *14*, 2707. (b) Reimer, K. J.; Shaver, A. *J. Organomet. Chem.* **1975**, *93*, 239. (c) Herrmann, W. A.; Huber, M. *Chem. Ber.* **1978**, *111*, 3124. (d) Herrmann, W. A.; Huber, M. *J. Organomet. Chem.* **1977**, *140*, 55. (e) Herrmann, W. A.; Reiter, B.; Huber, M. *J. Organomet. Chem.* **1977**, *139*, C4.

(14) Piper, T. S.; Wilkinson, G. *J. Inorg. Nucl. Chem.* **1956**, *3*, 104.

(15) A portion of this work has been communicated: Hubbard, J. L.; McVicar, W. K. *J. Am. Chem. Soc.* **1986**, *108*, 6422.

pendence of the reaction on a fresh Cu surface is shown by the fact that no reaction occurs in the absence of Cu and by the fact that the reaction is inhibited when the Cu becomes coated with hydrocarbon residues. The homo- or heterogeneous nature of the CH_2 insertion into the Cr–halide bond at or near the Cu surface remains a matter of speculation.[16] The sluggishness of the reaction when carried out in benzene is consistent with operation of a polar mechanism, perhaps reflecting the importance of the ionic character of the metal–halide bond. Interestingly, no reaction is observed when $(\eta^5\text{-}C_5H_5)Cr(NO)_2{}^+BF_4{}^-$ (**5**)[17] is treated with CH_2N_2, in both the presence and absence of Cu powder.

Our experiments indicate that metal chlorides and bromides convert to halomethyl products in similar reaction times but that metal iodide conversion to iodomethyl products is more sluggish. The complete conversion of $(\eta^5\text{-}C_5H_5)Cr(NO)_2I$ (**1c**) to $(\eta^5\text{-}C_5H_5)Cr(NO)_2CH_2I$ (**2c**) requires 3–4 times more CH_2N_2 and Cu powder compared to similar-scale reactions of the Cl or Br analogues. Fortunately, the formation of **2c** and **4c** is essentially quantitative from the treatment of **2a** or **4a** in a THF/NaI slurry (eq 2).

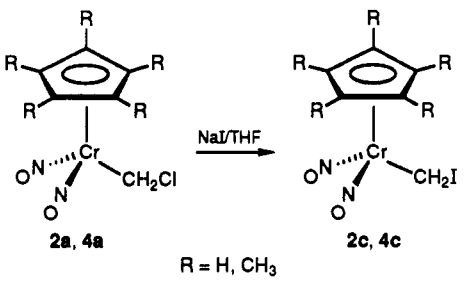

(2)

The entire group of $(\eta^5\text{-}C_5R_5)Cr(NO)_2CH_2X$ complexes can endure prolonged exposure to air, both in the solid state and as solutions in common organic solvents. They can be sublimed in vacuo between 50 and 80 °C with only modest decomposition. Mass spectrometry analysis shows a low-intensity molecular ion for all the complexes, with the base peak corresponding to loss of halide (vide infra).

The spectral characteristics for the new halomethyl complexes and their derivatives are shown in Table I. The halomethyl complexes show a single ^1H NMR resonance for the $\eta^5\text{-}C_5H_5$ or $\eta^5\text{-}C_5Me_5$ ligand. The single resonance for the CH_2X ligand shifts steadily to higher field as X changes Cl → Br → I. The ^{13}C NMR spectra also show a similar upfield shift for the CH_2 carbon resonance. The $^1J_{C\text{-}H}$ value of 149 Hz for the chloromethyl group of **2a** is characteristic of a normal primary alkyl chloride[18] and is only slightly larger than the $^1J_{C\text{-}H}$ value of 132 Hz that we observe for the $(\eta^5\text{-}C_5H_5)Cr(NO)_2CH_3$ complex. Labinger has commented on the relatively large $^1J_{C\text{-}H}$ values for the α-carbons of L_nMCH_2OR complexes and their L_nMCH_3 analogues.[18c]

Inspection of the ν_{NO} values for the complexes helps establish the donor properties of the halomethyl ligands.

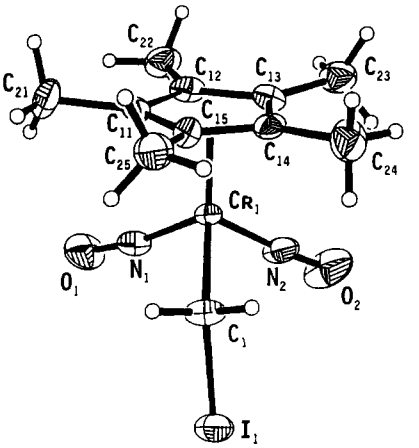

Figure 1. Molecular structure of **4c** giving the atom-labeling scheme. Non-hydrogen atoms are shown as 40% thermal ellipsoids. Hydrogen atoms are shown as small spheres.

In hexane solution, the ν_{NO} values for the chloromethyl complex **2a** (1792, 1690 cm^{-1}) lie between those for the chloride complex **1a** (1815, 1709 cm^{-1}) and $(\eta^5\text{-}C_5H_5)Cr(NO)_2CH_3$ (1786, 1684 cm^{-1}), suggesting the halomethyl group to be slightly less σ-donating than a methyl ligand. There is no significant variation of ν_{NO} as a function of the halide substituent.

A single-crystal X-ray diffraction study on $(\eta^5\text{-}C_5Me_5)Cr(NO)_2CH_2I$ (**4c**) reveals the structural aspects of the new chromium–halomethyl complexes. Fractional coordinates and equivalent isotropic displacement factors are given in Table II, and selected bond distances and bond angles are given in Tables III and IV, respectively. As seen in Figure 1, the molecule adopts a "piano-stool" geometry, similar to that found for **1a**.[19] The iodomethyl ligand is oriented nearly symmetrically in the mirror plane of the $(\eta^5\text{-}C_5Me_5)Cr(NO)_2$ moiety, with the iodide anti to the $\eta^5\text{-}C_5Me_2$ ring: the torsion angle (ring centroid)–Cr–C(1)–I(1) is 174.8°. The Cr–C(1)–I(1) bond angle is 115.1 (5)°, indicating the geometry at C(1) to be nearly tetrahedral. The Cr–C(1) distance of 2.093 (11) Å is similar to Cr–CH_3 bonds of several Cr(III)–methyl and –halomethyl complexes[10h,20] and is in the range of many Cr(0)–carbene bond distances.[21] Simple Cr^0–C single-bond distances are expected to fall in the range of 2.20–2.24 Å.[22] Thus, the shorter than expected Cr–C(1) distance may be a structural indication of some sp^2 character for the C(1) carbon, similar to the short Fe–C bond observed in the analogous $(\eta^5\text{-}C_5H_5)Fe(CO)(PPh_3)CH_2OR$ complex (eq 3).[23] The C(1) atom of

$$(\eta^5\text{-}C_5H_5)(CO)(PPh_3)Fe{-}CH_2{-}OR \leftrightarrow (\eta^5\text{-}C_5H_5)(CO)(PPh_3)Fe{=}CH_2{}^+OR^-$$

$$(\eta^5\text{-}C_5Me_5)(NO)_2Cr{-}CH_2{-}I \leftrightarrow (\eta^5\text{-}C_5Me_5)(NO)_2Cr{=}CH_2{}^+I^- \quad (3)$$

the iodomethyl ligand is only 2.91 Å from C(15), the

(16) (a) Chang, S.-C.; Kafafi, Z. H.; Hauge, R. H.; Billups, W. E.; Margrave, J. L. *J. Am. Chem. Soc.* **1987**, *109*, 4508. (b) Pettit, R.; Brady, R. C. *J. Am. Chem. Soc.* **1980**, *102*, 6181. (c) Muetterties, E. L.; Stein, J. *Chem. Rev.* **1979**, *21*, 479. (d) Yates, P. *J. Am. Chem. Soc.* **1952**, *74*, 5376. (d) Loggenberg, P. M.; Carlton, L.; Copperthwaite, R. G.; Hutchings, G. J. *J. Chem. Soc., Chem. Commun.* **1987**, 541. (e) Zheng, C.; Apeloig, Y.; Hoffmann, R. *J. Am. Chem. Soc.* **1988**, *110*, 749–774.

(17) (a) Regina, F. J.; Wojcicki, A. *Inorg. Chem.* **1980**, *19*, 3803. (b) Legzdins, P.; Martin, D. T.; Nurse, C. R.; Wassink, B. *Organometallics* **1983**, *2*, 1238.

(18) (a) Günther, H. *NMR Spectroscopy: An Introduction*; Wiley: New York, 1980. (b) Carhart, R. E.; Roberts, J. D. *Org. Magn. Reson.* **1971**, *3*, 139. (c) Labinger, J. *J. Organomet. Chem.* **1980**, *187*, 287.

(19) (a) Carter, O. L.; McPhail, A. T.; Sim, G. A. *J. Chem. Soc. A* **1966**, 1095. (b) Greenhough, T.; Kolthammer, B. W. S.; Legzdins, P.; Trotter, J. *Acta Crystallogr., Sect. B* **1980**, *B36*, 795.

(20) Noh, S. K.; Heintz, R. A.; Theopold, K. H. *Organometallics* **1989**, *8*, 2071.

(21) Kirtley, S. W. In *Comprehensive Organometallic Chemistry*; Wilkinson, G., Stone, F. G. A., Abel, E. W., Eds.; Pergamon Press: New York, 1982; Vol. 3.

(22) Distances for Cr^{II}–CH_3 bond lengths in quadruply bonded Cr dimers fall in the 2.21–2.24-Å range: (a) Cotton, F. A.; Koch, S. *Inorg. Chem.* **1978**, *17*, 2021. (b) Cotton, F. A.; Koch, S.; Millar, M. *Inorg. Chem.* **1978**, *17*, 2087.

(23) Chou, C.-K.; Miles, D. L.; Bau, R.; Flood, T. C. *J. Am. Chem. Soc.* **1978**, *100*, 7271.

nearest skeletal atom of the η^5-C_5Me_5 ligand. The η^5-C_5Me_5 ligand is symmetrically bound to the metal, with an average Cr–C distance of 2.21 Å and Cr–centroid distance of 1.86 Å. The nitrosyl ligands are essentially linear (average ∠Cr–N–O = 172.3°), representing a formal NO^+ mode of coordination. Within experimental error, the Cr–N–O angles are comparable to those found for **1a**.

Halide Abstraction. Our attempts to generate the $(\eta^5\text{-}C_5H_5)(NO)_2Cr{=}CH_2^+$ complex from the reaction of **2a** with $AgBF_4$ in CD_2Cl_2 gave a surprising result (eq 4).

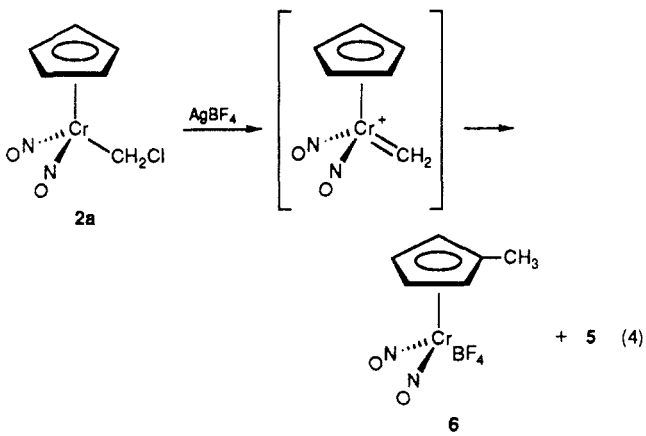

When the reaction is monitored by ^1H NMR spectroscopy over the period of several hours, the signals of **2a** disappear and new signals appear at δ 5.89 (m), 5.80 (t), 5.77 (t), 5.71 (t), 5.62 (t), 2.07 (s), and 2.04 (s). After 4 h, **2a** is completely gone, as are the peaks at δ 5.77 and 2.07. The peak at δ 5.89 becomes a sharp singlet and corresponds to the $(\eta^5\text{-}C_5H_5)Cr(NO)_2{}^+BF_4{}^-$ (**5**)[17] species (as compared to the product formed when **1a** is treated with excess $AgBF_4$ in CD_2Cl_2). The peaks at δ 5.71, 5.62, and 2.04 are identified as the $(\eta^5\text{-}C_5H_4Me)Cr(NO)_2{}^+BF_4{}^-$ (**6**) species (as compared to authentic material generated by treating $(\eta^5\text{-}C_5H_4Me)Cr(NO)_2Cl$ (**7**) with $AgBF_4$ in CD_2Cl_2). Integration of these peaks versus an internal standard shows **6** to be formed in ca. 90% yield from **2a**, with **5** being produced in ca. 5% yield. The spectral assignments of **5** and **6** are further confirmed by their conversion and subsequent ^1H NMR and IR identification as their neutral halide derivatives **1a** and **7**.[24] While we can presently only speculate about the nature of the species giving the transient signals at δ 5.88 (m), 5.77 (t), and 2.07 (s), it is possible that it is a η^5-C_5H_4Me complex containing Ag^+ together with the weakly coordinating BF_4^- counterion or solvent ligands. Reed and co-workers have recently reported the presence of halide-bridged adducts in silver salt metathesis reactions of $(\eta^5\text{-}C_5H_5)Fe(CO)_2I$.[25] Unfortunately, we have been unable to generate these signals upon treatment of **7** with $AgBF_4$ in CD_2Cl_2.

Treatment of a CD_2Cl_2 solution of **2a** with $AgBF_4$ in the presence of a 10-fold molar excess of cyclohexene shows no detectable formation of norcarane. This evidence shows that methylene migration to the η^5-C_5H_5 ligand is strongly preferred over intermolecular cyclopropanation. Under similar conditions, $(\eta^5\text{-}C_5H_5)Fe(CO)_2CH_2Cl$ shows no methylene migration to the η^5-C_5H_5 ligand, with cyclopropanation being the preferred mode of reactivity.[26]

Treatment of $(\eta^5\text{-}C_5H_4Me)Cr(NO)_2CH_2Cl$ (**8**) with $AgBF_4$ in CH_2Cl_2 followed by PPN^+Cl^- addition leads to the isolation of a 9:1 mixture of the 1,2- and 1,3-Me_2Cp products $(\eta^5\text{-}C_5H_3Me_2)Cr(NO)_2Cl$ (**9a,b** in a 1:1.2 ratio) and complex **7** (eq 5). The combined yield of $(\eta^5\text{-}C_5R_5)Cr(NO)_2Cl$ products from **8** is 84%. In contrast, methylene migration to the η^5-C_5Me_5 ligand does not occur when $(\eta^5\text{-}C_5Me_5)Cr(NO)_2CH_2Cl$ (**4a**) is treated with $AgBF_4$. When the reaction is followed by ^1H NMR spectroscopy in CD_2Cl_2 (eq 6), it is seen that **4a** reacts with $AgBF_4$ in the presence of a 10-fold excess of cyclohexene to give low yields of norcarane (≤5%). It is possible that the increased donor ability of the η^5-C_5Me_5 ring stabilizes the transient $(\eta^5\text{-}C_5Me_5)Cr(NO)_2{=}CH_2^+$ species enough to increase the probability of the cyclopropanation reaction in this case.

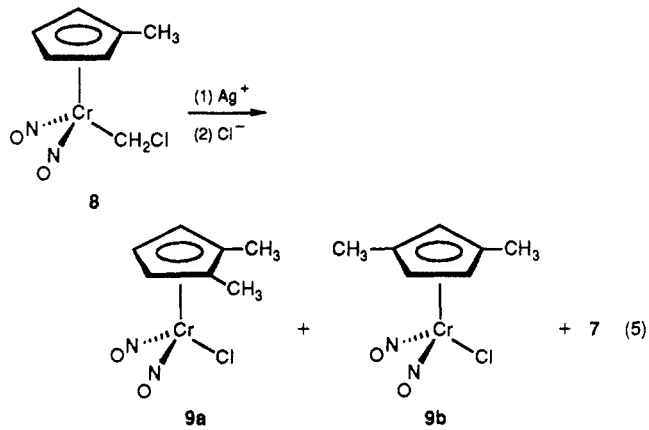

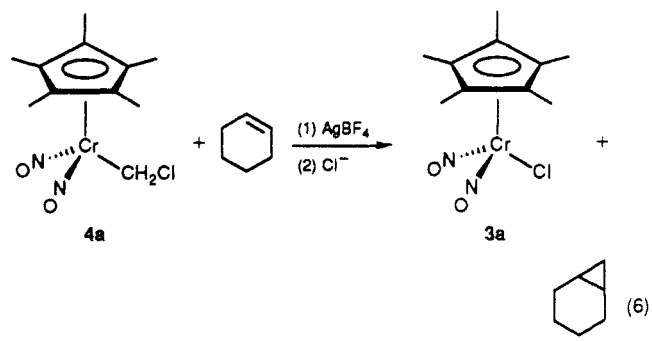

The intramolecular nature of the methylene migration was established by deuterium-labeling experiments. As summarized in Scheme I, treatment of equimolar amounts of **8** and **2a**-d_2 (or **8**-d_2 and **2a**) with $AgBF_4$ in CH_2Cl_2 results in no crossing of the deuterium label.

Halide Fragmentation in the Mass Spectrum. For each of the $(\eta^5\text{-}C_5R_5)Cr(NO)_2CH_2X$ complexes, the intensity of the fragment corresponding to halide loss is consistently high. The *m/e* 191 fragment, which arises from loss of halide from $(\eta^5\text{-}C_5H_5)Cr(NO)_2CH_2X$, cannot be differentiated between the $(\eta^5\text{-}C_5H_5)Cr(NO)_2{=}CH_2^+$ ion and the $(\eta^5\text{-}C_5H_4Me)Cr(NO)_2^+$ ion. However, the presence of a hydrocarbon fragment at *m/e* 79 corresponds to the $C_5H_4CH_3$ species, thus providing evidence for methylene

(24) There are now numerous examples of complexes containing weakly coordinating ligands (e.g., BF_4^-, PF_6^-, RX); see ref 17 and the following: (a) Beck, W. A.; Schloter, K. *Z. Naturforsch., B* **1978**, *33B*, 1214. (b) Sünkel, K.; Urban, G.; Beck, W. *J. Organomet. Chem.* **1985**, *290*, 231. (c) Legzdins, P.; Martin, D. T. *Organometallics* **1983**, *2*, 1785. (d) Hersh, W. H. *J. Am. Chem. Soc.* **1985**, *107*, 4599. (e) Winter, C. H.; Veal, W. R.; Garner, C. M.; Arif, A. M.; Gladysz, J. A. *J. Am. Chem. Soc.* **1989**, *111*, 4766 and references therein.

(25) Liston, D. J.; Lee, Y. J.; Scheidt, W. R.; Reed, C. A. *J. Am. Chem. Soc.* **1989**, *111*, 6643.

(26) Jolly, P. W.; Pettit, R. *J. Am. Chem. Soc.* **1966**, *88*, 5044.

(27) (a) Hall, M. B.; Kolthammer, B. W. S.; Morris-Sherwood, B. J. *Inorg. Chem.* **1981**, *20*, 2771. (b) Hubbard, J. L. Ph.D. Thesis, University of Arizona, 1982.

(28) (a) Lin, G.-Y.; Constable, A. G.; McCormick, F. B.; Strouse, C. E.; Eisenstein, O.; Gladysz, J. A. *J. Am. Chem. Soc.* **1982**, *104*, 4865. (b) Herrmann, W. A.; Hubbard, J. L.; Bernal, I.; Korp, J. D.; Haymore, B. L.; Hillhouse, G. L. *Inorg. Chem.* **1984**, *23*, 2978.

Table I. Spectroscopic Data for New $(\eta^5\text{-}C_5R_5)Cr(NO)_2CH_2X$ Complexes

complex	^1H NMR, δ ($CDCl_3$)	^{13}C NMR, δ ($CDCl_3$)	IR, cm^{-1} (ν_{NO})	CI mass spectrum, m/e (intens)
$(\eta^5\text{-}C_5H_5)Cr(NO)_2CH_2Cl$ (**2a**)	5.52 (s, 5 H, C_5H_5) 4.26 (2, 2 H, CH_2Cl)	100.4 (C_5H_5) 45.1 (CH_2Cl) {$^1J_{C-H}$ = 149 Hz}	1792 vs, 1690 vs[a]	[M + 1] 227 (3%) [M - Cl] 191 (100%) [C_5H_4Me] 79 (2%)
$(\eta^5\text{-}C_5H_5)Cr(NO)_2CH_2Br$ (**2b**)	5.52 (s, 5 H, C_5H_5) 4.02 (s, 2 H, CH_2Br)	100.7 (C_5H_5) 35.8 (CH_2Br)	1800 vs, 1698 vs[a]	[M + 1] 271 (1%) [M - Br] 191 (100%) [C_5H_4Me] 79 (3%)
$(\eta^5\text{-}C_5H_5)Cr(NO)_2CH_2I$ (**2c**)	5.51 (s, 5 H, C_5H_5) 3.30 (s, 2 H, CH_2I)	101.3 (C_5H_5) 3.3 (CH_2I)	1795 vs, 1693 vs[a]	[M + 1] 333 (14%) [M - I] 191 (100%) [C_5H_4Me] 79 (2%)
$(\eta^5\text{-}C_5Me_5)Cr(NO)_2CH_2Cl$ (**4a**)	3.84 (s, 2 H, CH_2Cl) 1.78 (s, 15 H, C_5Me_5)	109.0 (C_5Me_5) 50.6 (CH_2Cl) 9.1 (C_5Me_5)	1767 vs, 1670 vs[b]	[M + 1] 297 (3%) [M - Cl] 261 (100%)
$(\eta^5\text{-}C_5Me_5)Cr(NO)_2CH_2Br$ (**4b**)	3.60 (s, 2 H, CH_2Br) 1.77 (s, 15 H, C_5Me_5)	108.8 (C_5Me_5) 41.1 (CH_2Br) 9.1 (C_5Me_5)	1767 vs, 1671 vs[b]	[M + 1] 341 (5%) [M - Br] 261 (100%)
$(\eta^5\text{-}C_5Me_5)Cr(NO)_2CH_2I$ (**4c**)	2.81 (s, 2 H, CH_2I) 1.76 (s, 15 H, C_5Me_5)	108.8 (C_5Me_5) 8.8 (C_5Me_5) 6.4 (CH_2I)	1771 vs, 1675 vs[b]	[M + 1] 389 (12%) [M - I] 261 (94%)
$(\eta^5\text{-}C_5H_4Me)Cr(NO)_2CH_2Cl$ (**8**)	5.36 (t, 2 H, C_5H_4Me) 5.28 (t, 2 H, C_5H_4Me) 4.23 (s, 2 H, CH_2Cl) 2.01 (s, 3 H, C_5H_4Me)	115.7, 100.1 100.0 (C_5H_4Me) 45.9 (CH_2Cl) 12.6 (C_5H_4Me)	1783 vs, 1676 vs[c]	[M + 1] 241 (10%) [M - Cl] 205 (100%) [$C_5H_3Me_2$] 93 (12%) [C_5H_4Me] 79 (5%)
$(\eta^5\text{-}C_5H_5)Cr(NO)_2CH_2OTs$ (**10**)	7.75 (d, 2 H, OTs) 7.30 (d, 2 H, OTs) 5.45 (s, 5 H, C_5H_5) 5.03 (s, 2 H, CH_2OTs) 2.40 (s, 3 H, OTs)	143.9, 133.4 (OTs) 129.5, 127.9, 21.5 (OTs) 99.7 (C_5H_5) 76.3 (CH_2OTs)	1798 vs, 1697 vs[a]	[M + 1] 363 (30%) [M - OTs] 191 (100%) [C_5H_4Me] 79 (44%)
$(\eta^5\text{-}C_5H_5)Cr(NO)_2CH_2CN$ (**11**)	5.57 (s, 5 H, C_5H_5) 1.54 (s, 2 H, CH_2CN)	128.6 (CH_2CN) 100.7 (C_5H_5) -11.3 (CH_2CN)	1790 vs, 1682 vs[c] ν_{CN} 2194 w	[M + 1] 218 (100%)
$(\eta^5\text{-}C_5H_5)Cr(NO)_2CH_2OCH_3$ (**12**)	5.42 (s, 5 H, C_5H_5) 4.95 (s, 2 H, CH_2OMe) 3.25 (s, 3 H, CH_2OMe)	99.4 (C_5H_5) 80.3 (CH_2OMe) 60.1 (CH_2OMe)	1783 sh, 1775 vs, 1679 sh, 1674 vs[b]	[M + 1] 223 (11%) [M - OCH_3] 191 (100%) [C_5H_4Me] 79 (2%)
$(\eta^5\text{-}C_5Me_5)Cr(NO)_2CH_2OCH_3$ (**13**)	4.45 (s, 2 H, CH_2OCH_3) 3.25 (s, 3 H, CH_2OCH_3) 1.73 (s, 15 H, C_5Me_5)	107.8 (C_5Me_5) 86.8 (CH_2OCH_3) 60.5 (CH_2OCH_3) 9.0 (C_5Me_5)	1757 sh, 1747 vs, 1669 sh, 1662 vs[b]	[M + 1] 293 (100%) [M - NO] 262 (54%) [M - OCH_3] 261 (15%)
$(\eta^5\text{-}C_5Me_5)Cr(NO)_2CH_2OEt$ (**14**)	4.51 (s, 2 H, CH_2OEt) 3.36 (q, 2 H, OCH_2CH_3) 1.73 (s, 15 H, C_5Me_5) 1.14 (t, 3 H, OCH_2CH_3)	107.8 (C_5Me_5) 83.8 (CH_2OEt) 67.7 (OCH_2CH_3) 15.4 (OCH_2CH_3) 9.0 (C_5Me_5)	1756 s, 1747 vs, 1659 s, 1652 vs[b]	[M + 1] 307 (100%) [M - OCH_2CH_3] 261 (19%)
$(\eta^5\text{-}C_5H_5)Cr(NO)_2CH_2PPh_3^+BPh_4^-$ (**15b**)	7.6-7.9 (m, 15 H, PPh_3)[d] 7.32-6.75 (m, 20 H, BPh_4) 5.79 (s, 5 H, C_5H_5) 2.22 (s, 2 H, CH_2PPh_3) {$^1J_{HP}$ = 13.4 Hz}	164.4, 136.3 (BPh_4)[d] 125.5, 125.9 (BPh_4) 134.2, 132.9 (PPh_3) 130.2, 124.5 (PPh_3) 101.6 (C_5H_5) -5.0 (CH_2PPh_3)	1781 vs, 1652 vs[c]	

[a] Hexane. [b] Cyclohexane. [c] KBr. [d] NMR spectrum for **15b** in acetone-d_6.

migration in the gas phase. The m/e 79 fragment is not detected in the spectra of simple $(\eta^5\text{-}C_5H_5)Cr(NO)_2X$ complexes. Furthermore, this peak is shifted to m/e 81 for **2a**-d_2, supporting its assignment as the $C_5H_4CD_2H$ species. Similarly, the mass spectrum of **8** shows a fragment at m/e 93, representing the formation of the $C_5H_3Me_2$ species. For **8**-d_2, this peak is shifted to m/e 95. The m/e 93 fragment is not present in the mass spectrum of **7**. For the $(\eta^5\text{-}C_5Me_5)Cr(NO)_2CH_2X$ complexes we assign the m/e 261 peak as the $(\eta^5\text{-}C_5Me_5)Cr(NO)_2{=}CH_2^+$ species, since no methylene migration is observed in this case. There is no evidence in the mass spectrum for the C_5Me_4Et species at m/e 149.

Methylene Migration. The driving force for the intramolecular methylene migration most likely involves the extensive competition for d-π electron density around the $Cr(NO)_2$ functional group. It is well recognized that the nitrosyl ligands of the $Cr(NO)_2$ group stabilize the metal d^6 electrons more than the carbonyl ligands of the isoelectronic $Fe(CO)_2$ group.[24] Thus, the CH_2 ligand in the $(\eta^5\text{-}C_5H_5)Cr(NO)_2{=}CH_2^+$ species will be significantly more electrophilic than in the corresponding $(\eta^5\text{-}C_5H_5)Fe(CO)_2{=}CH_2^+$ complex. Terminal alkylidene ligands are known to be sensitive to the presence of strong π-acceptor ligands such as NO, adopting coordination geometries so as to minimize their competition for metal d-π electron density.[25] Given a favorable geometry, it is possible to envision the intramolecular electrophilic attack of the electron-deficient CH_2 ligand on the filled p-π orbitals of the cyclopentadienyl ligand (A). The X-ray structural analysis for **4c** shows that the iodomethyl carbon (C(1)) is only 2.91 Å from the nearest skeletal ring carbon (C(15)). A similar geometry can be reasonably assumed in **2a-c**, which actually undergo the methylene migration reaction.

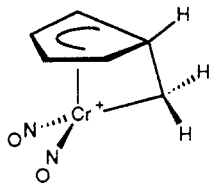

A

Halide Substitution Reactions. Reaction of **2a** with $AgOSO_2C_8H_4CH_3$ (AgOTs) results in the formation of $(\eta^5\text{-}C_5H_5)Cr(NO)_2CH_2OTs$ (**10**) in 73% yield. Protonation of **10** with excess CF_3CO_2H (TFA) or $HBF_4{\cdot}Et_2O$ produces **6** together with nearly equal amounts of **5** and CH_3OTs (eq 7). Even though the selectivity toward migration is

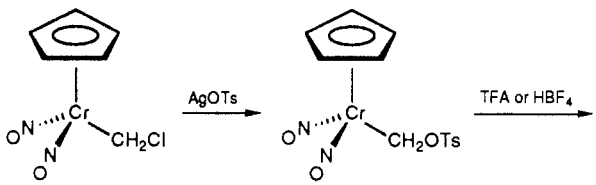

2a **10**

$$\mathbf{6} + \mathbf{5} + CH_3OTs \quad (7)$$

reduced, this result shows that the migration reaction is not dependent on the presence of Ag^+. The mass spectrum of **10** is also consistent with methylene migration in the gas phase, showing the predominance of the m/e 191 fragment and the presence of the C_5H_4Me fragment at m/e 79. The appearance of **5** and CH_3OTs in eq 8 corresponds

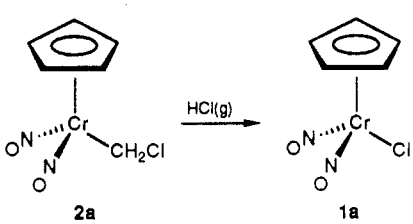

2a **1a**

$$+ CH_3Cl \quad (8)$$

to acid cleavage of the Cr–C bond, similar to previous reports for the production of **5** upon treating $(\eta^5\text{-}C_5H_5)Cr(NO)_2CH_3$ with HBF_4.[17a] Exposure of **10** in $CDCl_3$ to small amounts of anhydrous HCl leads to the formation of **1a**, **2a**, CH_3OTs, and CH_3Cl. Treatment of **2a** with excess anhydrous HCl gives essentially quantitative conversion to **1a** and CH_3Cl (eq 8). Apparently, the presence of the coordinating anion (Cl^-) suppresses the methylene migration process.

Halide exchange with exogenous X^- is quite facile in the $(\eta^5\text{-}C_5H_5)Cr(NO)_2CH_2X$ complexes. As mentioned earlier, treatment of Cr–chloromethyl complexes with a large excess of I^- gives virtually quantitative conversion to the iodomethyl derivatives. When equimolar amounts of $PPh_3{=}N{=}PPh_3{}^+Cl^-$ ((PPN)Cl) and **2b** are allowed to react in $CDCl_3$ at room temperature, equilibrium is reached within 6 h with **2a** as the predominant species (eq 9). Under similar conditions, **2a** is favored over **2c** (eq 10).

Surprisingly, halogen exchange does not occur under free radical/photolytic conditions. Solutions of **2a** and CBr_4 (20-fold excess) in $CDCl_3$ remain unchanged after several hours of exposure to a water-cooled medium-pressure discharge lamp (Pyrex filter). Solutions of **2b** in CCl_4 are similarly unaffected by irradiation at ambient temperatures.[29]

(29) $(\eta^5\text{-}C_5R_5)Fe(CO)_2CH_2X$ complexes are extremely reactive to halogen exchange under photolytic conditions: Hubbard, J. L.; McVicar, W. K. Unpublished results.

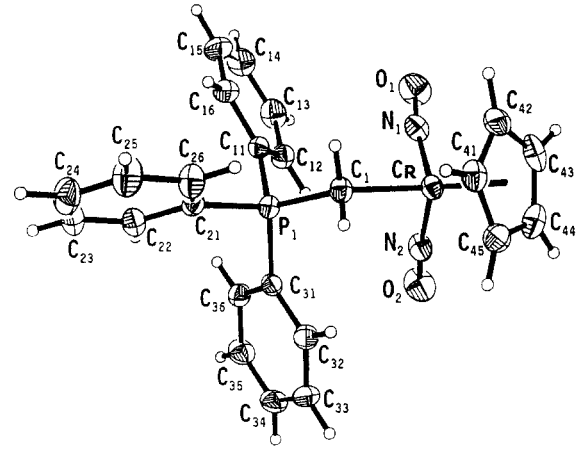

Figure 2. Molecular structure of the cationic species of **15b** giving the atom-labeling scheme. Non-hydrogen atoms are shown as 40% thermal ellipsoids. Hydrogen atoms are shown as small spheres.

Scheme I

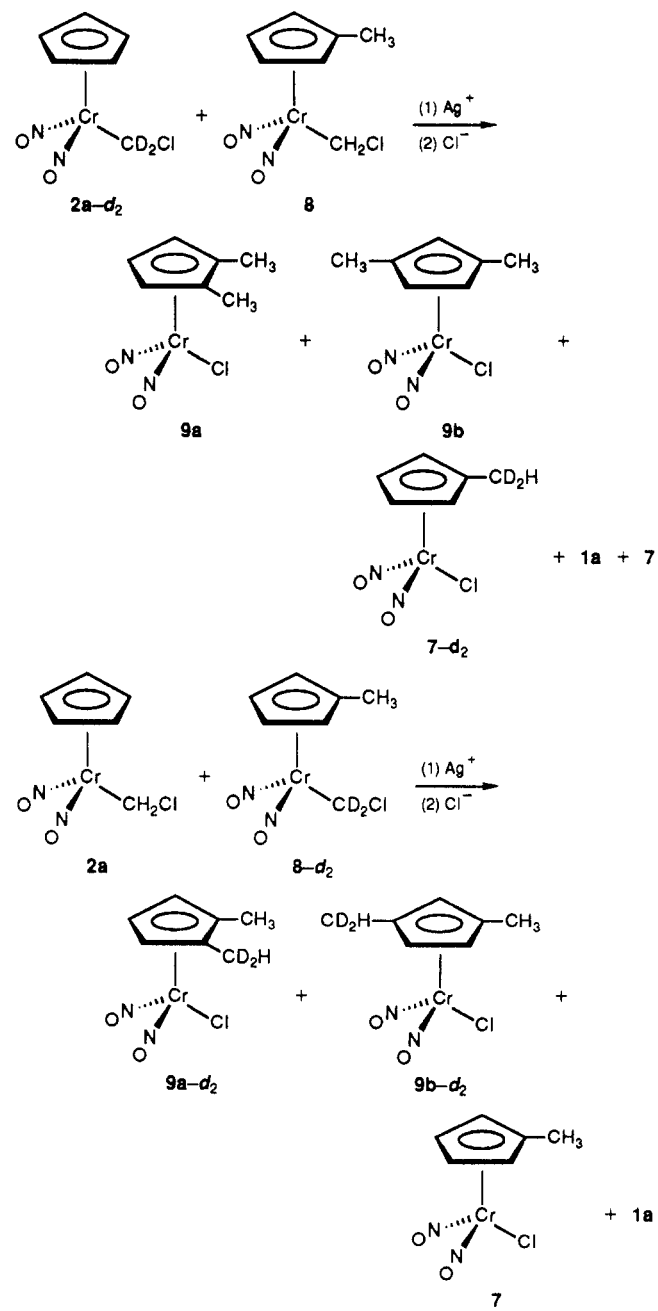

(9)

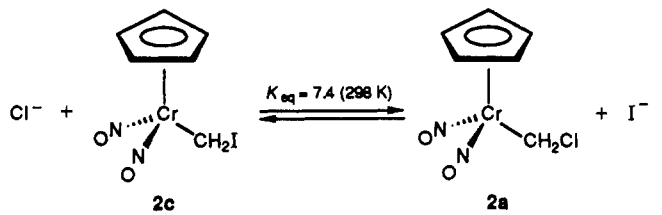

(10)

Cyanide replaces the bromide of **2b** irreversibly to give the corresponding stable cyanomethyl derivative **11** in 79% yield (eq 11). Protonation of **11** by anhydrous HCl in

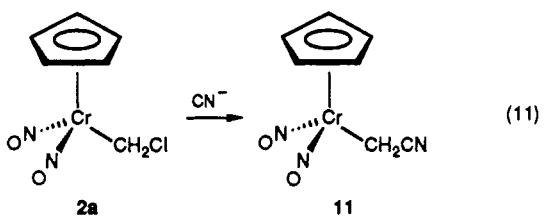

(11)

$CDCl_3$ leads to the formation of **5** and CH_3CN. In contrast to the case for the halomethyl complexes, the mass spectral fragmentation pattern of **11** shows the molecular ion to be the base peak. The *m/e* 191 peak (corresponding to loss of CN^-) and the *m/e* 79 peak (corresponding to the $C_5H_4CH_3$ species) are absent in the spectrum of the cyanomethyl complex, supporting our earlier argument that the appearance of the *m/e* 79 fragment is related to the fragmentation of the α-substituent.

Treatment of **2b** or **4b** with excess NaOMe in refluxing MeOH gives excellent conversion to the corresponding methoxymethyl derivatives **12** and **13**. Treatment of the halomethyl precursors with NaOEt in EtOH at 65 °C results in extensive decomposition. The $(\eta^5\text{-}C_5Me_5)Cr(NO)_2CH_2OEt$ complex (**14**) can be prepared by treatment of **2b** with excess TlOEt in EtOH (eq 12).

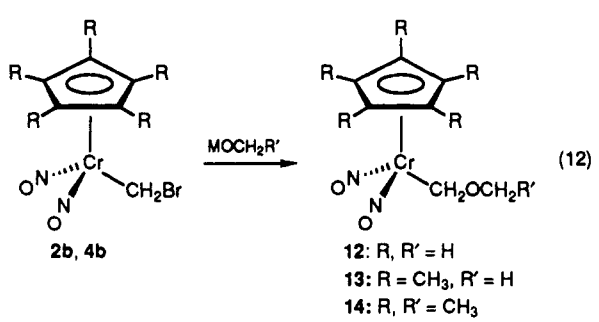

(12)

The alkoxymethyl derivatives are air-stable, olive green oils or solids. When dissolved in $CDCl_3$, **12** reacts with anhydrous HCl to form primarily **1a** and CH_3OCH_3. Only traces of **7** are detected, indicating methylene migration to be a low-yield process in this case. Surprisingly, **12**, **13**, and **14** show no reaction with TMSOTf ($Si(CH_3)_3SO_3CF_3$). Side-by-side control reactions of $(\eta^5\text{-}C_5H_5)Fe(CO)_2CH_2OCH_3$ with TMSOTf show the formation of $CH_3OSi(CH_3)_3$, $(\eta^5\text{-}C_5H_5)Fe(CO)_2^+$, and $(\eta^5\text{-}C_5H_5)Fe(CO)_2(\eta^2\text{-}C_2H_4)^+$.[30] Complexes **12** and **13** react with $ISi(CH_3)_3$ in $CDCl_3$ within 5 min to give **2c** and **4c**, respectively, as the only observed organometallic products. Similar treatment of **14** gives a mixture of **4c** and **3c**.

Table II. Atomic Coordinates (×10⁴) and Equivalent Isotropic Displacement Parameters (Å × 10³) for Compound 4c

	x	*y*	*z*	*U*(eq)[a]
I(1)	2238 (1)	767 (1)	2886 (1)	61 (1)
Cr(1)	-1107 (2)	178 (2)	2472 (2)	32 (1)
C(1)	765 (11)	-532 (11)	2559 (12)	44 (5)
N(1)	-831 (10)	1236 (11)	1545 (10)	47 (4)
O(1)	-824 (11)	1943 (11)	853 (10)	84 (5)
N(2)	-957 (10)	1088 (12)	3542 (10)	61 (5)
O(2)	-961 (12)	1742 (14)	4269 (11)	113 (6)
C(11)	-2314 (12)	-916 (12)	1361 (10)	39 (4)
C(12)	-3103 (12)	-158 (12)	1988 (1)	45 (5)
C(13)	-2968 (12)	-504 (12)	3072 (11)	43 (5)
C(14)	-2041 (13)	-1494 (13)	3061 (11)	47 (5)
C(15)	-1679 (12)	-1707 (12)	2040 (10)	36 (4)
C(21)	-2341 (17)	-834 (16)	180 (10)	71 (7)
C(22)	-4008 (14)	828 (15)	1602 (13)	67 (6)
C(23)	-3700 (14)	-32 (16)	3994 (12)	68 (6)
C(24)	-1645 (17)	-2197 (15)	4000 (11)	72 (7)
C(25)	-866 (14)	-2770 (14)	1673 (12)	62 (6)

[a] Equivalent isotropic *U* defined as one-third of the trace of the orthogonalized U_{ij} tensor.

Table III. Bond Lengths (Å) for Compound 4c

I(1)-C(1)	2.127 (11)	N(1)-O(1)	1.179 (14)
Cr(1)-N(1)	1.689 (13)	C(11)-C(12)	1.423 (18)
Cr(1)-C(11)	2.232 (12)	C(11)-C(21)	1.517 (17)
Cr(1)-C(13)	2.218 (12)	C(12)-C(22)	1.510 (18)
Cr(1)-C(15)	2.220 (13)	C(13)-C(23)	1.505 (18)
Cr(1)-C(1)	2.093 (11)	C(14)-C(24)	1.482 (18)
Cr(1)-N(2)	1.702 (13)	N(2)-O(2)	1.176 (14)
Cr(1)-C(12)	2.184 (12)	C(11)-C(15)	1.389 (17)
Cr(1)-C(14)	2.214 (13)	C(12)-C(13)	1.445 (18)
		C(13)-C(14)	1.451 (19)
		C(14)-C(15)	1.387 (17)
		C(15)-C(25)	1.517 (18)

The mass spectrum of **12** shows the fragmentation of the $-OCH_3$ substituent to give the *m/e* 191 species as the base peak. The presence of the *m/e* 79 peak again indicates that methylene migration occurs in the gas phase. In comparison, the mass spectra of **13** and **14** show the base peak to be the molecular ion. The *m/e* 261 fragment, arising from loss of the -OR substituent, is only 15–19% of the intensity of the molecular ion.

The nitrosyl IR features for the alkoxymethyl derivatives **12–14** are somewhat more complicated than those usually observed for dinitrosyl piano-stool complexes. The symmetric and asymmetric stretching bands are each split by 7–10 cm^{-1} when the complexes are examined in low-polarity solvents such as hexane, cyclohexane, and isooctane. The increased bandwidths in polar solvents such as CH_2Cl_2 prevent the resolution of the split bands. Similar splittings are observed in the metal–carbonyl IR bands of other $(\eta^5\text{-}C_5R_5)M(CO)_2R$ complexes and are attributed to the presence of conformational isomers.[31] In the new Cr–alkoxymethyl complexes, the relative intensities within the split symmetric and asymmetric bands are strongly tem-

(30) (a) Kegley, S. E.; Brookhart, M.; Husk, G. R. *Organometallics* **1982**, *1*, 760. (b) Cutler, A; Ehnholt, D.; Giering, P.; Lennon, S.; Raghu, A.; Rosen, M.; Rosenblum, M.; Tancrede, J.; Wells, D. *J. Am. Chem. Soc.* **1976**, *98*, 3495. (c) Davison, A.; McFarlane, W.; Pratt, W.; Wilkinson, G. *J. Chem. Soc.* **1962**, 3653.

(31) (a) Stanley, K.; Baird, M. C. *J. Am. Chem. Soc.* **1975**, *97*, 4292. (b) Blackburn, B. K.; Davies, S. G.; Whittaker, M. *J. Am. Chem. Soc., Chem. Commun.* **1987**, 1344. (c) Nakayawa, H.; Morimasa, K.; Kushi, Y.; Yoneda, H. *Organometallics* **1988**, *7*, 458. (d) Blackburn, K. L.; Bromley, L.; Davies, S. G.; Whittaker, M.; Jones, R. H. *J. Chem. Soc., Perkin Trans. 2* **1989**, 1143. (e) Cotton, F. A.; Marks, T. J. *J. Am. Chem. Soc.* **1969**, *91*, 7523.

Table IV. Bond Angles (deg) for Compounds 4c

N(1)-Cr(1)-C(1)	97.3 (5)	O(2)-N(2)-Cr(1)	174.4 (11)
N(2)-Cr(1)-N(1)	98.6 (6)	C(15)-C(11)-Cr(1)	71.3 (7)
C(11)-Cr(1)-N(1)	91.1 (5)	C(21)-C(11)-Cr(1)	127.4 (9)
C(12)-Cr(1)-C(1)	145.8 (5)	C(21)-C(11)-C(15)	131.7 (13)
C(12)-Cr(1)-N(2)	113.8 (5)	C(13)-C(12)-Cr(1)	72.1 (7)
C(13)-Cr(1)-C(1)	131.8 (5)	C(22)-C(12)-Cr(1)	123.6 (10)
C(13)-Cr(1)-N(2)	89.3 (5)	C(22)-C(12)-C(13)	123.7 (13)
C(13)-Cr(1)-C(12)	38.3 (5)	C(14)-C(13)-Cr(1)	70.7 (7)
C(14)-Cr(1)-N(1)	152.8 (5)	C(23)-C(13)-Cr(1)	127.4 (10)
C(14)-Cr(1)-C(11)	61.8 (5)	C(23)-C(13)-C(14)	127.3 (13)
C(14)-Cr(1)-C(13)	38.2 (5)	C(15)-C(14)-Cr(1)	72.0 (7)
C(15)-Cr(1)-N(1)	120.8 (5)	C(24)-C(14)-Cr(1)	126.3 (10)
C(15)-Cr(1)-C(11)	36.4 (4)	C(24)-C(14)-C(15)	127.1 (14)
C(15)-Cr(1)-C(13)	62.7 (5)	C(14)-C(15)-Cr(1)	71.5 (7)
Cr(1)-C(1)-I(1)	115.1 (5)	C(25)-C(15)-Cr(1)	130.3 (9)
O(1)-N(1)-Cr(1)	170.2 (11)	C(25)-C(15)-C(14)	125.5 (12)
C(12)-C(11)—Cr(1)	69.4 (7)	N(2)-Cr(1)-C(1)	95.8 (5)
C(15)-C(11)-C(12)	106.4 (11)	C(11)-Cr(1)-C(1)	110.2 (5)
C(21)-C(11)-C(12)	121.8 (13)	C(11)-Cr(1)-N(2)	150.9 (5)
C(11)-C(12)Cr(1)	73.1 (7)	C(12)-Cr(1)-N(1)	94.9 (5)
C(13)-C(12)-C(11)	109.9 (11)	C(12)-Cr(1)-C(11)	37.6 (5)
C(22)-C(12)-C(11)	126.3 (13)	C(13)-Cr(1)-N(1)	129.3 (5)
C(12)-C(13)-Cr(1)	69.6 (7)	C(13)-Cr(1)-C(11)	63.7 (5)
C(14)-C(13)-C(12)	104.1 (11)	C(14)-Cr(1)-C(1)	94.7 (5)
C(23)-C(13)-C(12)	128.4 (13)	C(14)-Cr(1)-N(2)	104.3 (6)
C(13)-C(14)-Cr(1)	71.0 (7)	C(14)-Cr(1)-C(12)	62.6 (5)
C(15)-C(14)-C(13)	108.8 (11)	C(15)-Cr(1)-C(1)	84.9 (4)
C(24)-C(14)-C(13)	123.9 (14)	C(15)-Cr(1)-N(2)	140.2 (6)
C(11)-C(15)-Cr(1)	72.3 (7)	C(15)-Cr(1)-C(12)	61.5 (5)
C(14)-C(15)-C(11)	110.8 (12)	C(15)-Cr(1)-C(14)	36.5 (5)
C(25)-C(15)-C(11)	123.2 (12)		

perature-dependent, suggestive of a conformer equilibrium process. A full analysis of this behavior is the subject of a forthcoming paper.[32]

Reaction of **2c** with PPh_3 occurs in boiling ethanol to give the stable cationic ylide complex $(\eta^5\text{-}C_5H_5)Cr(NO)_2CH_2PPh_3^+I^-$ (**15a**). The complex is conveniently obtained as the BPh_4^- salt (**15b**), from which X-ray-quality crystals can be obtained (eq 13). The formation of **15a**

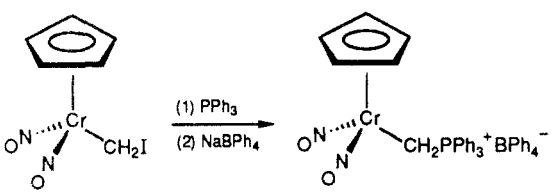

2c **15b** (13)

from **2c** is similar to the reaction of alkyl iodides with PPh_3 to give quaternary phosphonium salts. The formation of $(\eta^5\text{-}C_5H_5)Fe(CO)_2CH_2PPh_3^+I^-$ by treating $(\eta^5\text{-}C_5H_5)Fe(CO)_2CH_2OMe$ with $[PPh_3H]I$ is believed to proceed through the intermediate $(\eta^5\text{-}C_5H_5)Fe(CO)_2CH_2I$ complex.[33] Several other cationic ylide complexes are known to form from the addition of tertiary phosphines to halomethyl precursors.[34]

Consistent with considerable ylide ($^-CH_2P^+Ph_3$) character for the CH_2PPh_3 ligand, the IR spectrum of **15b** reveals that the positive charge in the cation is remote from the metal–dinitrosyl functional group. The ν_{NO} frequencies (in KBr) for **15b** are actually lower than those of the parent complex **2c**, indicating the CH_2PPh_3 ligand to be more donating than the CH_2I ligand. A similar conclusion is drawn from the fact that the ^1H NMR methylene resonance for the CH_2PPh_3 ligand (δ 2.22) comes at considerably higher field than that for the CH_2I ligand (δ 3.30). The downfield chemical shift of the quaternary P atom of **15b** is also consistent with considerable positive charge at the phosphorus atom[35] and is similar to that for other complexes containing the CH_2PPh_3 ligand.[36]

Table V. Atomic Coordinates ($\times 10^4$) and Equivalent Isotropic Displacement Parameters (Å $\times 10^3$) for Compound 15b

	x	y	z	U(eq)[a]
Cr	4675 (1)	3606 (1)	8265 (1)	39 (1)
N(1)	3364 (3)	4062 (1)	7952 (2)	50 (1)
O(1)	2347 (3)	4322 (1)	7769 (2)	80 (1)
N(2)	5086 (3)	3877 (1)	9205 (2)	51 (1)
O(2)	5234 (3)	4023 (2)	9871 (2)	83 (1)
C(1)	6186 (3)	3988 (1)	7747 (2)	40 (1)
P(1)	6719 (1)	4682 (1)	7994 (1)	35 (1)
C(11)	5328 (3)	5176 (1)	7726 (2)	37 (1)
C(12)	4541 (3)	5343 (2)	8260 (2)	46 (1)
C(13)	3503 (4)	5724 (2)	8030 (3)	63 (2)
C(14)	3239 (4)	5943 (2)	7271 (3)	70 (2)
C(15)	3984 (4)	5769 (2)	6736 (3)	68 (2)
C(16)	5028 (4)	5391 (2)	6959 (2)	53 (1)
C(21)	7976 (3)	4903 (2)	7445 (2)	39 (1)
C(22)	8621 (3)	5424 (2)	7608 (2)	49 (1)
C(23)	9544 (4)	5601 (2)	7178 (3)	60 (2)
C(24)	9835 (4)	5270 (2)	6585 (3)	67 (2)
C(25)	9205 (4)	4758 (2)	6418 (3)	69 (2)
C(26)	8281 (4)	4573 (2)	6845 (2)	55 (1)
C(31)	7466 (3)	4760 (1)	9033 (2)	37 (1)
C(32)	8121 (3)	4303 (2)	9462 (2)	46 (1)
C(33)	8741 (3)	4365 (2)	10256 (2)	57 (2)
C(34)	8696 (4)	4878 (2)	10633 (2)	59 (2)
C(35)	8074 (4)	5330 (2)	10214 (2)	56 (1)
C(36)	7463 (3)	5277 (2)	9417 (2)	45 (1)
C(41)	5253 (4)	2855 (2)	7615 (2)	49 (1)
C(42)	3859 (4)	2944 (2)	7393 (2)	59 (2)
C(43)	3326 (4)	2873 (2)	8092 (3)	64 (2)
C(44)	4391 (4)	2753 (2)	8713 (3)	62 (2)
C(45)	5589 (4)	2744 (2)	8426 (2)	55 (1)
B(1)	347 (4)	2294 (2)	34 (2)	38 (1)
C(51)	1304 (3)	2716 (1)	679 (2)	36 (1)
C(52)	2536 (3)	2917 (2)	540 (2)	46 (1)
C(53)	3443 (3)	3231 (2)	1089 (2)	52 (1)
C(54)	3156 (4)	3362 (2)	1811 (2)	55 (1)
C(55)	1956 (4)	3176 (2)	1978 (2)	49 (1)
C(56)	1054 (3)	2860 (1)	1422 (2)	41 (1)
C(61)	-48 (3)	2579 (2)	-856 (2)	38 (1)
C(62)	164 (3)	3139 (2)	-1042 (2)	47 (1)
C(63)	-245 (4)	3352 (2)	-1808 (2)	57 (2)
C(64)	-906 (4)	3015 (2)	-2422 (2)	58 (2)
C(65)	-1155 (4)	2467 (2)	-2257 (2)	56 (1)
C(66)	-740 (3)	2249 (2)	-1499 (2)	47 (1)
C(71)	-1142 (3)	2162 (2)	254 (2)	41 (1)
C(72)	-1942 (3)	2601 (2)	446 (2)	54 (1)
C(73)	-3229 (4)	2513 (2)	595 (2)	68 (2)
C(74)	-3783 (4)	1978 (3)	538 (2)	75 (2)
C(75)	-3050 (4)	1537 (2)	331 (2)	69 (2)
C(76)	-1744 (4)	1630 (2)	198 (2)	53 (1)
C(81)	1289 (3)	1728 (2)	33 (2)	40 (1)
C(82)	2053 (4)	1626 (2)	-545 (2)	54 (1)
C(83)	2960 (4)	1184 (2)	-493 (3)	74 (2)
C(84)	3131 (5)	808 (2)	132 (3)	83 (2)
C(85)	2400 (5)	893 (2)	710 (3)	75 (2)
C(86)	1514 (4)	1340 (2)	666 (2)	54 (1)

[a] Equivalent isotropic U defined as one-third of the trace of the orthogonalized U_{ij} tensor.

(32) Hubbard, J. L.; McVicar, W. K. Manuscript in preparation.
(33) (a) Pelling, S.; Moss, J. R.; Botha, C. *J. Chem. Soc., Dalton Trans.* **1983**, 1495. (b) Reger, D. L.; Culbertson, E. C. *J. Organomet. Chem.* **1977**, *132*, 69.
(34) (a) Moss, J. R.; Niven, M. L.; Stretch, P. M. *Inorg. Chim. Acta* **1986**, *119*, 177. (b) Moss, J. R.; Engelte, C.; Nassimbeni, C. R.; Reid, G.; Spiers, J. C. *J. Organomet. Chem.* **1986**, *315*, 255. (c) Klein, H. F.; Hammer, R. *Angew. Chem., Int. Ed. Engl.* **1977**, *15*, 42. (d) Hofmann, L.; Werner, H. *J. Organomet. Chem.* **1985**, *289*, 141. (e) Werner, H.; Paul, W.; Wolf, J.; Steinmetz, M.; Zolk, R.; Müller, G.; Steigelmann, O.; Riede, J. *Chem. Ber.* **1989**, *122*, 1061. (f) Steinmetz, M.; Werner, H. *J. Organomet. Chem.* **1989**, *369*, 309. (g) Werner, H.; Hofmann, L.; Ziegler, M. L.; Zahn, T. *Organometallics* **1986**, *5*, 510. (h) Werner, H.; Feser, R.; Paul, W.; Hofmann, L. *J. Organomet. Chem.* **1981**, *219*, C29. (i) Guerchais, V.; Astruc, D.; Nunn, C. M.; Cowley, A. H. *Organometallics* **1990**, *9*, 1036.
(35) Crutchfield, M. M.; Dungan, C. H.; Letcher, J. H.; Mark, V.; Van Wazer, J. R. *Top. Phosphorus Chem.* **1967**, *5*, 1.

Table VI. Bond Lengths (Å) for Compound 15b

Cr–N(1)	1.696 (3)	Cr–N(2)	1.701 (3)
Cr–C(1)	2.115 (3)	Cr–C(41)	2.236 (4)
Cr–C(42)	2.197 (4)	Cr–C(43)	2.177 (4)
Cr–C(44)	2.194 (4)	Cr–C(45)	2.224 (4)
N(1)–O(1)	1.174 (4)	N(2)–O(2)	1.172 (3)
C(1)–P(1)	1.748 (3)	P(1)–C(11)	1.800 (3)
P(1)–C(21)	1.806 (3)	P(1)–C(31)	1.787 (3)
C(11)–C(12)	1.387 (4)	C(11)–C(16)	1.381 (5)
C(12)–C(13)	1.370 (5)	C(13)–C(14)	1.372 (6)
C(14)–C(15)	1.366 (6)	C(15)–C(16)	1.367 (5)
C(21)–C(22)	1.388 (5)	C(21)—C(26)	1.377 (5)
C(22)–C(23)	1.368 (5)	C(23)–C(24)	1.363 (6)
C(24)–C(25)	1.365 (6)	C(25)–C(26)	1.370 (5)
C(31)–C(32)	1.389 (5)	C(31)–C(36)	1.388 (5)
C(32)–C(33)	1.379 (5)	C(33)–C(34)	1.378 (6)
C(34)–C(35)	1.361 (6)	C(35)–C(36)	1.379 (5)
C(41)–C(42)	1.385 (5)	C(41)–C(45)	1.385 (5)
C(42)–C(43)	1.422 (6)	C(43)–C(44)	1.368 (6)
C(44)–C(45)	1.393 (5)	B(1)–C(51)	1.637 (5)
B(1)–C(61)	1.638 (5)	B(1)–C(71)	1.647 (5)
B(1)–C(81)	1.637 (5)	C(51)–C(52)	1.393 (4)
C(51)–C(56)	1.393 (4)	C(52)–C(53)	1.379 (5)
C(53)–C(54)	1.365 (5)	C(54)–C(55)	1.368 (5)
C(55)–C(56)	1.383 (5)	C(61)–C(62)	1.385 (5)
C(61)–C(66)	1.404 (5)	C(62)–C(63)	1.383 (5)
C(63)–C(64)	1.372 (6)	C(64)–C(65)	1.359 (6)
C(65)–C(66)	1.377 (5)	C(71)–C(72)	1.394 (5)
C(71)–C(76)	1.387 (5)	C(72)–C(73)	1.385 (5)
C(73)–C(74)	1.375 (7)	C(74)–C(75)	1.363 (6)
C(75)–C(76)	1.395 (5)	C(81)–C(82)	1.398 (5)
C(81)–C(86)	1.402 (5)	C(82)–C(83)	1.375 (6)
C(83)–C(84)	1.373 (7)	C(84)–C(85)	1.367 (6)
C(85)–C(86)	1.372 (6)		

Table VII. Bond Angles (deg) for Compound 15b

N(2)–Cr–N(1)	94.4 (1)	C(1)—Cr–N(1)	100.1 (1)
C(1)–Cr–N(2)	100.9 (1)	C(41)–Cr–N(1)	127.7 (1)
C(41)–Cr–N(2)	137.2 (2)	C(41)–Cr–C(1)	80.9 (1)
C(42)–Cr–N(1)	94.8 (1)	C(42)–Cr–N(2)	153.1 (2)
C(42)–Cr–C(1)	102.3 (1)	C(42)–Cr–C(41)	36.4 (1)
C(43)–Cr–N(1)	92.4 (2)	C(43)–Cr–N(2)	116.4 (2)
C(43)–Cr–C(1)	139.6 (1)	C(43)–Cr–C(41)	61.5 (1)
C(43)–Cr–C(42)	37.9 (1)	C(44)–Cr–N(1)	122.8 (2)
C(44)–Cr–N(2)	92.0 (2)	C(44)–Cr–C(1)	134.1 (1)
C(44)–Cr–C(41)	60.9 (1)	C(44)–Cr–C(42)	61.9 (2)
C(44)–Cr–C(43)	36.5 (2)	C(45)–Cr–N(1)	153.0 (1)
C(45)–Cr–N(2)	102.4 (2)	C(45)–Cr–C(1)	97.3 (1)
C(45)–Cr–C(41)	36.2 (1)	C(45)–Cr–C(42)	61.2 (1)
C(45)–Cr–C(43)	61.2 (2)	C(45)–Cr–C(44)	36.8 (1)
O(1)–N(1)–Cr	170.8 (3)	O(2)–N(2)–Cr	171.6 (3)
P(1)–C(1)–Cr	120.4 (2)	C(11)–P(1)–C(1)	111.3 (2)
C(21)–P(1)–C(1)	110.8 (2)	C(21)–P(1)–C(11)	105.7 (2)
C(31)–P(1)–C(1)	112.3 (2)	C(31)–P(1)–C(11)	109.0 (2)
C(31)–P(1)–C(21)	107.4 (1)	C(12)–C(11)–P(1)	122.3 (3)
C(16)–C(11)–P(1)	118.7 (3)	C(16)–C(11)–C(12)	119.1 (3)
C(13)–C(12)–C(11)	120.1 (4)	C(14)–C(13)–C(12)	120.0 (4)
C(15)–C(14)–C(13)	120.1 (4)	C(16)—C(15)–C(14)	120.4 (4)
C(15)–C(16)–C(11)	120.2 (4)	C(22)–C(21)–P(1)	119.9 (3)
C(26)–C(21)–P(1)	121.3 (3)	C(26)–C(21)–C(22)	118.8 (3)
C(23)–C(22)–C(21)	120.2 (4)	C(24)–C(23)–C(22)	120.4 (4)
C(25)–C(24)–C(23)	120.0 (4)	C(26)–C(25)–C(24)	120.4 (4)
C(25)–C(26)–C(21)	120.2 (4)	C(32)–C(31)–P(1)	119.9 (3)
C(36)–C(31)–P(1)	121.4 (3)	C(36)–C(31)—C(32)	118.7 (3)
C(33)–C(32)–C(31)	120.3 (4)	C(34)–C(33)–C(32)	120.2 (4)
C(35)–C(34)–C(33)	119.9 (4)	C(36)–C(35)–C(34)	120.6 (4)
C(35)–C(36)–C(31)	120.4 (4)	C(42)–C(41)–Cr	70.3 (2)
C(45)–C(41)–Cr	71.4 (2)	C(45)–C(41)–C(42)	108.6 (3)
C(41)–C(42)–Cr	73.3 (2)	C(43)–C(42)–Cr	70.3 (2)
C(43)–C(42)–C(41)	106.9 (4)	C(42)–C(43)–Cr	71.8 (2)
C(44)–C(43)–Cr	72.4 (2)	C(44)–C(43)–C(42)	107.9 (3)
C(43)–C(44)–Cr	71.1 (2)	C(45)–C(44)–Cr	72.8 (2)
C(45)–C(44)–C(43)	108.5 (4)	C(41)–C(45)–Cr	72.4 (2)
C(44)–C(45)–Cr	70.5 (2)	C(44)–C(45)–C(41)	108.0 (4)
C(61)–B(1)–C(51)	111.8 (3)	C(71)–B(1)–C(51)	113.0 (3)
C(71)–B(1)–C(61)	103.9 (3)	C(81)–B(1)–C(51)	103.9 (3)
C(81)–B(1)–C(61)	111.0 (3)	C(81)–B(1)–C(71)	113.4 (3)
C(52)–C(51)–B(1)	120.4 (3)	C(56)–C(51)–B(1)	124.9 (3)
C(56)–C(51)–C(52)	114.4 (3)	C(53)–C(52)–C(51)	123.2 (3)
C(54)–C(53)–C(52)	120.3 (3)	C(55)–C(54)–C(53)	118.9 (3)
C(56)–C(55)–C(54)	120.3 (3)	C(55)–C(56)–C(51)	122.9 (3)
C(62)–C(61)–B(1)	126.0 (3)	C(66)–C(61)–B(1)	119.0 (3)
C(66)–C(61)–C(62)	114.9 (3)	C(63)–C(62)–C(61)	122.4 (4)
C(64)–C(63)–C(62)	121.0 (4)	C(65)–C(64)–C(63)	118.2 (4)
C(66)–C(65)–C(64)	121.2 (4)	C(65)–C(66)–C(61)	122.3 (4)
C(72)–C(71)–B(1)	120.7 (3)	C(76)–C(71)–B(1)	124.0 (3)
C(76)–C(71)–C(72)	115.1 (3)	C(73)–C(72)–C(71)	122.6 (4)
C(74)–C(73)–C(72)	120.3 (4)	C(75)–C(74)–C(73)	119.1 (4)
C(76)–C(75)–C(74)	120.1 (4)	C(75)–C(76)–C(71)	122.8 (4)
C(82)–C(81)–B(1)	123.1 (3)	C(86)–C(81)–B(1)	122.0 (3)
C(86)–C(81)–C(82)	114.6 (3)	C(83)–C(82)–C(81)	122.7 (4)
C(84)–C(83)–C(82)	120.8 (4)	C(85)–C(84)–C(83)	118.3 (4)
C(86)–C(85)–C(84)	121.0 (4)	C(85)–C(86)–C(81)	122.6 (4)

The molecular structure of **15b** as determined by X-ray diffraction is shown in Figure 2. Table V lists the atomic coordinates, and selected bond lengths and bond angles are listed in Tables VI and VII, respectively. The complex cation possesses an overall piano-stool geometry, with the P(1) atom lying nearly in the mirror plane of the (η^5-C_5H_5)$Cr(NO)_2$ moiety. The PPh_3 group is apparently oriented so as to minimize steric interaction with the η^5-C_5H_5 ligand: the (ring centroid)–Cr–C(1)–P(1) torsion angle is 170.4°. Even so, the Cr–C(2)–P(1) bond angle of 120.4 (2)° is 5° larger than the Cr–C(1)–I(1) angle found in **4c**. This increase is likely a manifestation of the greater steric demands of the PPh_3 group. For comparison, a ∠W–C–P angle of 119 (1)° is found in the (η^5-C_5Me_5)$W(CO)_3CH_2PPh_3^+$ complex ion;[34a,37] a very recent report shows ∠Fe–C–P in the (η^5-C_5Me_5)$Fe(CO)_2CH_2PPh_3^+$ cation to be 118.1°.[34i] The Cr–C(1) bond length of 2.115 (3) Å for **15b** compares closely to that found in **4c**. The P(1)–C(1) bond length of 1.748 (3) Å is intermediate between the 1.66-Å distance in $CH_2{=}PPh_3$[38] and the 1.80–1.85-Å range for a P—C single bond,[36] again indicating some residual ylide character for the CH_2PPh_3 ligand in complex **15b**. The C(41) atom of the η^5-C_5H_5 ligand is positioned over the Cr–C(1) bond, with a C(1)–C(41) distance of 2.91 Å. The average ∠Cr–N–O angle is 171.1°, corresponding to a linear, NO^+ mode of coordination. The coordination around P(1) is nearly tetrahedral. The average ∠C–B–C value of 109.5° in the BPh_4^- anion indicates normal tetrahedral geometry about the boron atom.

Concluding Remarks

The availability of this class of halomethyl complexes opens up a new avenue to study fundamental metal–carbon interactions. Especially interesting is the opportunity to examine the effects that extremely strong π-acceptor ligands have on the stability and reactivity of the metal–CH_2 moiety derived from the halomethyl precursors. Unlike previous studies on isoelectronic metal carbonyl/phosphine systems, the transient methylidene species generated from the new Cr–halomethyl or –alkoxymethyl complexes is shown to be so electrophilic that intramolecular methylene migration is preferred over intermolecular reactivity. The stability of the new chromium complexes permits the characterization of a variety of substitution reactions at the halomethyl carbon. The facile nature of halide exchange at the halomethyl carbon shows the importance of the $Cr{=}CH_2^+X^-$ resonance form for describing the halomethyl ligation. Indeed, we have determined the structure of a stable iodomethyl complex and a cationic ylide derivative, revealing the Cr—C bond to be somewhat shorter than expected for a simple Cr—C single bond. We are

(36) (a) Schmidbauer, H. *Angew. Chem., Int. Ed. Engl.* **1983**, *22*, 907–927. (b) Kaska, W. C. *Coord. Chem. Rev.* **1983**, *48*, 1–58.

(37) Engelter, C.; Moss, J. R.; Niven, M. L.; Nassimbeni, L. R.; Reid, G. *J. Organomet. Chem.* **1982**, *232*, C78.

(38) Bart, J. C. J. *Angew. Chem., Int. Ed. Engl.* **1968**, *7*, 730.

continuing to investigate the chemistry of the entire family of $(\eta^5\text{-}C_5R_5)M(NO)_2CH_2X$ complexes in order to better assess both the stabilization and reactivity of the metal–halomethyl bond.

Experimental Section

Standard Schlenk techniques were employed in all syntheses. The nitrogen reaction atmosphere was purified by passing through scavengers for water (Aquasorb, Mallinckrodt) and oxygen (Catalyst R3-11, Chemical Dynamics, South Plainfield, NJ). Reagent-grade solvents were purified by distillation from appropriate drying agents. The column chromatography supports used were Al_2O_3 (150 mesh, activity I, neutral, Aldrich; deactivated to Al_2O_3 (III) by addition of 6% H_2O w/w), SiO_2 (60–200 mesh, Baker), and Florisil (60–100 mesh, Fisher). Both SiO_2 and Florisil supports were activated by drying under 1×10^{-5} Torr vacuum for 24 h. Routine filtrations were performed through Analytical Filter Pulp (Schliesser and Schuller). Infrared spectra were recorded on a Perkin-Elmer 1430 spectrophotometer and were referenced to the 1601-cm^{-1} polystyrene stretch. The ^1H and ^{13}C NMR spectra were recorded on a Bruker WP-270 spectrometer at 270 and 67.9 MHz, respectively. Residual solvent peaks were used as internal standards (7.24 ppm (^1H) and 77.0 ppm (^{13}C) for $CDCl_3$, 7.15 ppm (^1H) and 128.0 ppm (^{13}C) for C_6H_6, 2.04 ppm (^1H) and 29.8 ppm (^{13}C) for acetone-d_6, 5.32 ppm (^1H) for CD_2Cl_2); phosphoric acid (85%) was the external reference for ^{31}P NMR spectroscopy. Mass spectra were obtained with a Finnigan 4610 mass spectrometer using electron impact (EI) or chemical ionization (CI, methane). Melting points were measured with a Mel-Temp device (Laboratory Devices) in open capillaries and are uncorrected. Combustion analyses were performed by Robertson Laboratories, Inc., Madison, NJ.

Diazomethane (CH_2N_2) was generated by using the "alcohol-free" method from Diazald (Aldrich).[39] *Caution*! Diazomethane is exceedingly toxic, and solutions have been known to explode unaccountably! All work must be carried out in a well-ventilated fume hood behind safety shields. The ethereal diazomethane was collected directly onto KOH pellets and was stored in a −60 °C dewar until use. The reservoir of CH_2N_2 was tapped with 0.5 mm i.d. Teflon cannula tubing (Rainin Corp.) and was pumped with a peristaltic pump (Haake-Buchler Model No. 426-2000) equipped with a 20-cm section of 1.6 mm i.d. Viton tubing (Cole-Parmer). A second piece of Teflon tubing delivered the CH_2N_2 solution to the vented reaction vessel through a rubber septum. Deuterated diazomethane was prepared from MNNG (Aldrich) in diethyl ether over KOD/D_2O in a two-phase reaction. Copper powder (electrolytic dust) was used as received from Fisher. (PPN)Cl ($Ph_3PNPPh_3^+Cl^-$) was prepared by literature methods;[40] (PPN)CN was prepared by metathesis with NaCN in H_2O, analogous to the procedure reported for the preparation of $(PPN)NO_2$.[41] $AgBF_4$, AgOTs, TMSOTf, $ISi(CH_3)_3$, TlOEt, $HBF_4{\cdot}Et_2O$, CBr_4, and $NaB(C_6H_5)_4$ were used as received from Aldrich.

The starting chlorides **1a**, **3a**, and **7** were prepared from NOCl and the corresponding $(\eta^5\text{-}C_5R_5)Cr(CO)_2NO$ precursors by following published procedures.[42] The bromide analogues **1b** and **3b** were prepared with use of NOBr in place of NOCl.[43] The iodide analogues **1c** and **3c** were prepared by repeated treatment of **1a** and **3a** with excess NaI in THF.[27a] The characterizations of **1b**, **1c**, **3b**, **3c**, and **7** are given here.

$(\eta^5\text{-}C_5H_5)Cr(NO)_2Br$ (1b). ^1H NMR ($CDCl_3$): δ 5.72. IR (KBr): 1820 vs, 1705 vs cm^{-1}. Mass spectrum (CI): [M + 1] *m/e* 258 (18%), [M − Br] *m/e* 177 (100%). Anal. Calcd for $C_5H_5N_2O_2BrCr$: C, 23.37; H, 1.96; N, 10.90. Found: C, 23.45; H, 2.03; N, 10.98.

$(\eta^5\text{-}C_5H_5)Cr(NO)_2I$ (1c). ^1H NMR ($CDCl_3$): δ 5.73. IR (Et_2O): ν_{NO} 1808 vs, 1709 vs cm^{-1}. Anal. Calcd for $C_5H_5N_2O_2ICr$: C, 19.75; H, 1.66; N, 9.22. Found: C, 19.88; H, 1.75; N, 9.34.

$(\eta^5\text{-}C_5Me_5)Cr(NO)_2Br$ (3b). ^1H NMR ($CDCl_3$): δ 1.84. $^{13}C\{^1H\}$ NMR ($CDCl_3$): δ 112.0 ($\eta^5\text{-}C_5Me_5$), δ 9.44 ($\eta^5\text{-}C_5Me_5$). IR (KBr): ν_{NO} 1770 vs, 1690 vs cm^{-1}. Mass spectrum (CI): [M + 1] *m/e* 328 (34%), [M − Br] *m/e* 247 (100%). Anal. Calcd for $C_{10}H_{15}N_2O_2BrCr$: C, 36.71; H, 4.62; N, 8.56. Found: C, 36.86; H, 4.75; N, 8.66.

$(\eta^5\text{-}C_5Me_5)Cr(NO)_2I$ (3c). ^1H NMR ($CDCl_3$): δ 1.91. IR (KBr): ν_{NO} 1785 vs, 1690 vs cm^{-1}. Anal. Calcd for $C_{10}H_{15}N_2O_2ICr$: C, 32.10; H, 4.04; N, 7.49. Found: C, 32.36; H, 4.15; N, 7.58.

$(\eta^5\text{-}C_5H_4Me)Cr(NO)_2Cl$ (7). ^1H NMR ($CDCl_3$): δ 5.55 (t, 2 H, $\eta^5\text{-}C_5H_4Me$), δ 5.36 (t, 2 H, $\eta^5\text{-}C_5H_4Me$), δ 2.04 (s, 3 H, $\eta^5\text{-}C_5H_4Me$). $^{13}C\{^1H\}$ NMR ($CDCl_3$): δ 121.6 (s, $\eta^5\text{-}C_5H_4Me$) δ 101.94 (broad, $\eta^5\text{-}C_5H_4Me$), δ 13.2 (s, $\eta^5\text{-}C_5H_4Me$). IR (KBr): ν_{NO} 1815 vs, 1691 vs cm^{-1}. Mass spectrum (EI): [M^+] *m/e* 226 (10%), [M − Cl] *m/e* 191 (100%), [$C_5H_4CH_3$] *m/e* 8%. Anal. Calcd for $C_8H_7N_2O_2ClCr$: C, 31.80; H, 3.11; N, 12.36. Found: C, 32.02; H, 3.22; N, 12.49.

Synthesis of $(\eta^5\text{-}C_5R_5)Cr(NO)_2CH_2X$. The formation of **2a** from CH_2N_2/Cu treatment of **1a** is typical for the synthesis of the entire series of chloro- and bromomethyl complexes. While the direct formation of iodomethyl derivatives from the parent iodides is possible, the reactions consistently required 2–5 times longer reaction times (i.e. a larger excess of CH_2N_2); passivation of the Cu powder (by polymethylene) after reaction times longer than 20–30 min necessitated filtration of the iodide/iodomethyl reaction mixtures into clean reaction tubes containing fresh Cu powder every 30 min until IR spectra showed complete conversion of the starting material. The iodomethyl complexes are most easily obtained by a Finkelstein-type conversion of chloromethyl complexes (vide infra).

$(\eta^5\text{-}C_5H_5)Cr(NO)_2CH_2Cl$ (2a). A Schlenk tube with a magnetic stirbar was charged with 0.20 g (0.94 mmol) of **1a**, 100 mL of Et_2O, and 5 g of Cu powder and was sealed with a septum fitted with the Teflon CH_2N_2 delivery cannula and a Teflon vent cannula. Ethereal diazomethane (ca. 1 M) was peristaltically pumped to the reaction vessel at the rate of ca. 20 drops/min for 20–30 min with vigorous stirring. Diazomethane addition was stopped after IR spectra showed no more starting halide, and stirring was continued for an additional 5 min to decompose any remaining CH_2N_2. The reaction mixture was filtered through a 2×4 cm plug of Al_2O_3 (I) into a clean Schlenk tube and the solvent removed in vacuo. Extraction of the residue with 30 mL of hexane followed by filtration through filter pulp, concentration to 15 mL, and crystallization at −40 °C gave 0.19 g (0.83 mmol, 88%) of green, air-stable **2a**. Anal. Calcd for $C_6H_7N_2O_2ClCr$: C, 31.81; H, 3.11; N, 12.36. Found: C, 31.65; H, 3.11; N, 12.12. Mp: 71–73 °C.

$(\eta^5\text{-}C_5H_5)Cr(NO)_2CH_2Br$ (2b) was isolated as green crystals from hexane at −40 °C and as a green oil at room temperature (93% yield from **1b**). Anal. Calcd for $C_6H_7N_2O_2CrBr$: C, 26.58; H, 2.58; N, 10.34. Found: C, 26.31; H, 2.47; N, 10.17.

$(\eta^5\text{-}C_5H_5)Cr(NO)_2CH_2I$ (2c). A THF solution (50 mL) containing **2a** (0.25 g, 1.1 mmol) and NaI (2.0 g, 13.3 mmol, excess) was stirred at room temperature for 48 h. After solvent removal in vacuo, the residue was extracted with hexane and filtered; **2c** was isolated as green crystals at −40 °C and a green oil at room temperature (0.35 g, 1.0 mmol, 95%). Anal. Calcd for $C_6H_7N_2O_2CrI$: C, 22.65; H, 2.20; N, 8.80. Found: C, 22.88; H, 2.42; N, 8.78.

$(\eta^5\text{-}C_5Me_5)Cr(NO)_2CH_2Cl$ (4a) was isolated as green crystals from hexane at −40 °C (93% yield from **3a**). Anal. Calcd for $C_{11}H_{17}N_2O_2ClCr$: C, 44.53; H, 5.73; N, 9.45. Found: C, 43.95; H, 5.80; N, 9.23. Mp: 122–123 °C.

$(\eta^5\text{-}C_5Me_5)Cr(NO)_2CH_2Br$ (4b) was isolated as green crystals from hexane at −40 °C (90% yield from **3b**). Anal. Calcd for $C_{11}H_{17}N_2O_2BrCr$: C, 38.82; H, 5.02; N, 8.21. Found: C, 38.87; H, 5.02; N, 8.37. Mp: 136–137 °C.

$(\eta^5\text{-}C_5Me_5)Cr(NO)_2CH_2I$ (4c). Green crystals were isolated in 95% yield from hexane at −40 °C by two successive treatments of **4a** with a 10-fold excess of NaI in THF. Anal. Calcd for $C_{11}H_{17}N_2O_2CrI$: C, 34.04; H, 4.38; N, 7.22. Found: C, 34.26; H, 4.19; N, 7.03. Mp: 145–146 °C.

(39) *Aldrichimica Acta* **1983**, *16*, 1.
(40) Ruff, J. K.; Schlientz, W. J. *Inorg. Synth.* **1974**, *15*, 84.
(41) Martinsen, A.; Songstad, J. *Acta Chem. Scand., Ser. A* **1977**, *A31*, 645.
(42) Legzdins, P.; Hoyano, J. K.; Malito, J. T. *Inorg. Synth.* **1978**, *18*, 126.
(43) Ratcliff, C. T.; Shreeve, J. M. *Inorg. Synth.* **1968**, *11*, 199.

(η^5-C_5H_4Me)$Cr(NO)_2CH_2Cl$ (8) was isolated as green crystals from hexane at −40 °C and a green oil at room temperature (90% yield from **7**). Anal. Calcd for $C_7H_9N_2O_2ClCr$: C, 34.93; H, 3.77; N, 11.64. Found: C, 35.01; H, 3.85; N, 11.81.

Treatment of 2a with $AgBF_4$. A mixture of **2a** (0.20 g, 0.9 mmol) and $AgBF_4$ (0.20 g, 1.0 mmol) in 50 mL of CH_2Cl_2 was vigorously agitated by magnetic stirring in darkness for 4 h. (PPN)Cl (1.1 g, 1.9 mmol) was added with continued stirring. After 0.5 h, the solvent was removed in vacuo and the residue was extracted with ether (3 × 30 mL). The combined extracts were concentrated to ca. 15 mL and cooled to −40 °C, giving 0.17 g of green, crystalline product that was characterized as a 5:1 mixture of **7** to **1a** (73% yield of **7** from **2a**).

This reaction was also investigated by ^1H NMR spectroscopy in CD_2Cl_2. A 5-mm NMR tube was charged with 5 mg of **2a**, 5 mg of $AgBF_4$, and 2 μL of C_6H_6 (an internal integration standard). CD_2Cl_2 (ca. 0.5 mL) was vacuum-transferred into the tube, and the tube was sealed with a torch. The initial ^1H NMR spectrum showed only the starting complex with the solvent peak and the C_6H_6 reference. The tube was periodically shaken over a period of 4 h and then centrifuged before measuring each subsequent ^1H NMR spectrum.

Treatment of 8 with $AgBF_4$. A Schlenk tube was charged with **8** (0.15 g, 0.6 mmol), $AgBF_4$ (0.12 g, 0.6 mmol), 50 mL of CH_2Cl_2, and a stirbar. The mixture was stirred vigorously for 4 h, and then (PPN)Cl (1.0 g, 1.7 mmol) was added. After 0.5 h the solvent was removed in vacuo and the residue extracted with ether (3 × 30 mL). The combined extracts were concentrated to 15 mL and cooled to −40 °C, giving 0.12 g of crystalline green product (green oil at room temperature). Analysis by ^1H NMR spectroscopy (including selective homonuclear decoupling experiments) showed the product to be a 1:1.2 mixture of 1,2- and 1,3-Me_2Cp isomers of (η^5-$C_5H_3Me_2$)$Cr(NO)_2Cl$ (**9a,b**, ca. 75% combined yield from **8**) and **7** (ca. 9% yield from **8**). ^1H NMR ($CDCl_3$) for **9a**: δ 5.38 (t, 1 H, H_a on 4-position); δ 5.31 (d, 2 H, (H_b, $H_{b'}$ on Cp 3,5-positions); J_{ab} = 3 Hz; δ 1.91 (s, 6 H, $C_5H_3Me_2$). ^1H NMR for **9b**: δ 5.21 (d, 2 H, H_a, $H_{a'}$ on the Cp 4,5-positions); δ 5.07 (m, 1 H, H_b on the Cp 2-position); δ 1.98 (s, 6 H, η^5-$C_5H_3Me_2$). IR for **9b** (CH_2Cl_2): ν_{NO} 1801 vs, 1694 vs cm^{-1}.

Reaction of 8/2a-d_2 or 8-d_2/2a Mixture with $AgBF_4$. A Schlenk tube containing a stirbar was charged with **8** (0.14 g, 0.6 mmol), **2a**-d_2, (0.13 g, 0.6 mmol), $AgBF_4$ (0.23 g, 1.2 mmol), and 20 mL of CH_2Cl_2. After the mixture was stirred in darkness for 5 h, (PPN)Cl (1.0 g, 1.7 mmol) dissolved in 10 mL of CH_2Cl_2 was added and stirring continued for 0.5 h. The solvent was removed in vacuo, and the crude residue was analyzed by ^1H NMR spectroscopy. The major organometallic products were the two isomers **9a,b** and **7**-d_2. The only other organometallic products detectable were small amounts of **7** and **1a** (similar to the results of adding $AgBF_4$ to **8** or **2a** (vide supra)), thus indicating no crossover of the deuterium label. The complex **7**-d_2 was generated and characterized independently by treating **2a**-d_2 with $AgBF_4$ followed by addition of (PPN)Cl. In a second experiment, the deuterium label was switched: equimolar amounts of **8**-d_2 and **2a** were treated together with $AgBF_4$. ^1H NMR spectra of the reaction residue showed no detectable amounts of **7**-d_2. After workup by chromatography on SiO_2 and crystallization from 1:1 hexane/CH_2Cl_2, both labeling reactions gave combined (η^5-C_5R_5)$Cr(NO)_2Cl$ product yields ≥80% (0.22–0.23 g of oily green residue).

Treatment of 4a with $AgBF_4$. A Schlenk flask with magnetic stirbar was charged with **4a** (0.15 g, 0.5 mmol), $AgBF_4$ (0.10 g, 0.5 mmol), and 40 mL of CH_2Cl_2. The mixture was stirred vigorously for 6 h, and then (PPN)Cl (0.86 g, 1.5 mmol) was added. After 0.5 h the solvent was removed in vacuo. ^1H NMR spectroscopy ($CDCl_3$) showed a considerable amount of a hydrocarbon-like material (δ 1.22, 0.86) and **3a** as the only organometallic product; **3a** was recovered in 90% yield after chromatography on SiO_2 with CH_2Cl_2 and recrystallization in 1:1 CH_2Cl_2/hexane at −40 °C. Repeating the procedure on an NMR-tube scale ($CDCl_3$) with a 10-fold excess of cyclohexene resulted in the formation of norcarane in approximately 5% yield.

Preparation of (η^5-C_5H_5)$Cr(NO)_2CH_2OSO_2C_6H_4CH_3$ (10). A Schlenk tube was charged with **2b** (0.40 g, 1.5 mmol), $AgOSO_2C_6H_4CH_3$ (0.79 g, 2.83 mmol), 40 mL of CH_2Cl_2, and a stirbar. The reaction mixture was stirred vigorously for 29 h in the dark. The reaction mixture was filtered to remove the AgBr precipitate, and the CH_2Cl_2 was removed in vacuo. The residue was taken up in a minimum of 2:1 hexane/CH_2Cl_2 and filtered a final time through filter pulp. Crystallization from 2:1 hexane/CH_2Cl_2 at −40 °C gave 0.41 g (1.1 mmol, 73%) of **10** as a green, microcrystalline solid. Anal. Calcd for $C_{13}H_{14}N_2O_5SCr$: C, 43.09; H, 3.87; N, 7.73. Found: C, 42.86; H, 4.01; N, 7.52. Mp: 103–105 °C dec.

Protonation of 10. Complex **10** (0.02 g) was dissolved in neat CF_3CO_2H or in HBF_4·Et_2O, resulting in a color change to dark brown over a 4-h period. The solvent was removed in vacuo, and the residue was extracted with $CDCl_3$: ^1H NMR spectroscopy showed the presence of **6** together with nearly equal amounts of **5** and $CH_3OSO_2C_6H_4CH_3$.

Preparation of (η^5-C_5H_5)$Cr(NO)_2CH_2CN$ (11). A Schlenk tube was charged with **2a** (0.26 g, 1.1 mmol), (PPN)CN (0.90 g, 1.6 mmol), 50 mL of CH_2Cl_2, and a stirbar. The mixture was stirred for 3 h and then poured directly onto a 2 × 10 cm column of Al_2O_3 (III) prepared in CH_2Cl_2. Elution with CH_2Cl_2 produced a green band. Solvent removal in vacuo and extraction of the residue with 50 mL of warm hexane was followed by filtration and concentration to 20 mL. Crystallization at −40 °C gave pure **11** (0.19 g, 0.9 mmol, 79%). Anal. Calcd for $C_7H_7N_3O_2Cr$: C, 38.72; H, 3.25; N, 19.35. Found: C, 39.01; H, 3.28; N, 19.13.

Reaction of 2a with Anhydrous HCl. A 5-mm NMR tube was charged with ca. 2 mg of **2a** and 0.5 mL of $CDCl_3$ with a trace of CH_2Cl_2 (as internal integral standard) and closed with a septum. After a starting spectrum was measured, the tube was opened and anhydrous HCl was briefly blown over the solution. A second ^1H NMR spectrum showed that **2a** had been converted to **1a** (δ 5.70) and CH_3Cl (δ 3.00) in over 95% yield (versus the internal CH_2Cl_2 reference).

Preparation of (η^5-C_5H_5)$Cr(NO)_2CH_2OCH_3$ (12). A Schlenk tube was charged with 0.14 g (0.52 mmol) of **2b**, 20 mL of 0.1 M $NaOCH_3$ in CH_3OH, and a stirbar. The mixture was heated to reflux for 75 min, and then the solvent was removed in vacuo. The residue was extracted in 25 mL of hexane and transferred to a 1 × 10 cm column of Al_2O_3 (III) prepared in hexane. Elution with 2:1 hexane/Et_2O produced an olive green band. Recrystallization from pentane at −40 °C gave 0.11 g (0.51 mmol, 98%) of **12** (crystals melt to an oil at room temperature). Anal. Calcd for $C_7H_{10}N_2O_3Cr$: C, 37.84; H, 4.54; N, 12.61. Found: C, 37.72; H, 4.59; N, 12.47.

Preparation of (η^5-C_5Me_5)$Cr(NO)_2CH_2OCH_3$ (13). The preparation followed the same procedure as for **12**. Complex **13** was isolated as brown crystals from −40 °C pentane in 95% yield. Anal. Calcd for $C_{12}H_{20}N_2O_3Cr$: C, 49.31; H, 6.90; N, 9.58. Found: C, 49.60; H, 6.92; N, 9.45. Mp: 45–46 °C.

Preparation of (η^5-C_5Me_5)$Cr(NO)_2CH_2OCH_2CH_3$ (14). A Schlenk tube was charged with 0.24 g (0.7 mmol) of **4b**, 0.5 mL (1.8 g, 7.1 mmol) of $TlOCH_2CH_3$, 30 mL of CH_3OH, and a stirbar. The reaction mixture was heated to 65 °C for 4 h, after which time a large amount of white precipitate had formed and the solution was deep blue-green. The alcohol was removed in vacuo and the oily residue transferred in a minimum of hexane to a 2 × 25 cm Al_2O_3 (III) column prepared in hexane. Elution with 200 mL of hexane produced the unreacted **4b** (0.04 g, 0.1 mmol, 16% recovery). Elution with 20:1 hexane/Et_2O produced a yellow-green band that gave 0.12 g (0.39 mmol, 66% based on recovered starting material) of **14** after recrystallization from pentane at −80 °C. Anal. Calcd for $C_{13}H_{22}N_2O_3Cr$: C, 50.98; H, 7.19; N, 9.15. Found: C, 51.14; H, 7.31; N, 9.08. Mp: 42–43 °C.

Protonation of 12. Approximately 5 mg of **12** was placed in a 5-mm NMR tube and dissolved in ca. 0.5 mL of $CDCl_3$. CH_2Cl_2 (1.0 μL) was added as an internal integration standard. After an initial ^1H NMR spectrum was measured, anhydrous HCl was briefly blown into the tube and the spectrum was remeasured. Over a period of 30 min the initial clear olive green color had changed to slightly cloudy bright green. The starting complex had been completely consumed, and CH_3OCH_3 was present in ca. 70% yield. Peaks for **7** were evident in ca. 5% yield.

Treatment of 12 and 13 with TMSOTf. Approximately 10 mg of alkoxymethyl complex **12** or **13** was placed in a Schlenk reaction bulb attached directly to a high-vacuum line. Several milliliters of TMSOTf was vacuum-transferred onto the complex at 77 K, and the mixture was allowed to melt to room temperature.

Table VIII. Crystal Data and Details of Data Collection for 4c and 15b

	4c	15b
empirical formula	$C_{11}H_{17}N_2O_2ICr$	$C_{48}H_{42}BN_2O_2PCr$
mol wt	388.2	772.6
cryst color	green	green
cryst size, mm	0.08 × 0.20 × 0.25	0.25 × 0.20 × 0.20
cryst syst	monoclinic	monoclinic
a, Å	10.366 (3)	10.038 (2)
b, Å	10.974 (2)	23.587 (4)
c, Å	12.818 (3)	17.150 (3)
α, deg	90.0	90.0
β, deg	90.81 (2)	102.35 (1)
γ, deg	90.0	90.0
V, Å^3	1458.1 (6)	3967 (1)
Z	4	4
d(calcd), g/cm^3	1.77	1.30
temp, °C	25	25
space group	$P2_1/a$	$P2_1/c$
radiation (wavelength, Å)	Mo Kα (0.71073)	Mo Kα (0.71073)
μ, cm^{-1}	28.55	3.3
scan type	θ–2θ	θ–2θ
scan range (2θ), deg	3–50	3–45
no. of rflns collected	2871	6997
no. of indep rflns	2575	6569
no. of rflns $I \geq 3\sigma$	1666	4635
R^a	0.075	0.048
$R_w{}^b$	0.069	0.054
data/param ratio	10.8	9.0
GOF	1.46	1.31
max Δ/σ	0.04	0.18
residual density, e/Å^3	1.57 (0.57 Å from I(1))	0.28

$^a R = \sum||F_o| - |F_c||/\sum|F_o|$. $^b R_w = [\sum w(|F_o| - |F_c|)^2/\sum w|F_o|^2]^{1/2}$.

The resulting clear olive green solutions were allowed to stand for 15 min, and then the mixture was taken to dryness in vacuo. ^{1}H NMR spectra of the residue in $CDCl_3$ showed only unreacted **11** and **12** in each case.

Treatment of 12, 13, and 14 with ISi(CH$_3$)$_3$. A 5-mm NMR tube containing ca. 5 mg of the alkoxymethyl complex dissolved in $CDCl_3$ was charged with ca. 5 μL of $ISi(CH_3)_3$. The NMR spectrum was measured within 1–2 min. For complexes **12** and **13**, **2c** was the only organometallic species detected. Complex **14** also reacted quickly with $ISi(CH_3)_3$, giving a mixture of **4c** and **3c** in a 3:1 ratio.

Preparation of (η^5-C$_5$H$_5$)Cr(NO)$_2$CH$_2$PPh$_3^+$BPh$_4^-$ (15b). A Schlenk tube was charged with 0.43 g (1.35 mmol) of **2c**, 0.39 g (1.5 mmol) of PPh_3, 40 mL of CH_3OH, and a stirbar. The mixture was heated to reflux for 4 h, after which time the ν_{NO} bands for the starting material had been completely replaced by a new set of ν_{NO} bands at slightly lower energy (KBr pellet). $NaBPh_4$ (0.92 g, 2.7 mmol) dissolved in a minimum of CH_3OH was added to the reaction mixture, causing an immediate precipitation of a bright green solid. Recrystallization of this solid from boiling acetone gave 0.53 g (0.7 mmol, 52%) of **15b** as analytically pure green prisms. Anal. Calcd for $C_{48}H_{42}N_2O_2BPCr$: C, 74.61; H, 5.48; N, 3.62. Found: C, 74.32; H, 5.27; N, 3.91. Mp >200 °C (darkens with dec).

X-ray Structure of 4c. A suitable crystal was fixed vertically on a glass fiber with epoxy cement and centered on a Nicolet R3m/v diffractometer with graphite-monochromated Mo Kα radiation (λ = 0.71073 Å). Autocentering indicated a primitive monoclinic cell; axial symmetry along the unique b axis was verified by photography. The centrosymmetric space group $P2_1/a$ was determined from the systematic absences in the data. No empirical absorption correction was applied. The structure was solved by Patterson methods. Remaining non-hydrogen atoms were located in subsequent difference Fourier maps. Hydrogen atoms were generated in idealized positions with fixed (0.08) thermal parameters. All computations used the SHELXTL PLUS package of programs (Siemens Corp., Madison, WI).

Table VIII provides the crystal, data collection, and refinement parameters. Fractional atomic coordinates and equivalent isotropic displacement parameters (Table II), bond lengths (Table III), and bond angles (Table IV) are also provided. Anisotropic displacement parameters, H atom coordinates, and structure factors are available as supplementary material.

X-ray Structure of 15b. A suitable crystal was fixed vertically in a sealed glass capillary and centered on a Nicolet R3m/v diffractometer with graphite-monochromated Mo Kα radiation (λ = 0.71073 Å). Autocentering indicated a primitive monoclinic cell; axial symmetry along the unique b axis was verified by photography. The centrosymmetric space group $P2_1/c$ was determined from the systematic absences in the data. No empirical absorption correction was applied. The structure was solved by direct methods. Remaining non-hydrogen atoms were located in subsequent difference Fourier maps. Hydrogen atoms were generated in idealized positions with fixed (0.08) thermal parameters. All computations used the SHELXTL PLUS package of programs (Siemens Corp., Madison, WI).

Table VIII provides the crystal, data collection, and refinement parameters. Fractional atomic coordinates and equivalent isotropic displacement parameters (Table V), bond lengths (Table VI), and bond angles (Table VII) are also provided. Anisotropic displacement parameters, H atom coordinates, and structure factors are available as supplementary material.

Acknowledgment. The donors of the Petroleum Research Fund, administered by the American Chemical Society, Research Corp., and most recently the National Science Foundation (Grant No. CHE-8901855) are all gratefully acknowledged for the support of this research over the past several years. In addition, we thank the University of Vermont and Utah State University for institutional support. The X-ray diffractometer was purchased with funds from the Vermont-EPSCoR program.

Supplementary Material Available: Full tables of the crystallographic data, hydrogen atom coordinates, and anisotropic displacement parameters for **4c** and **15b** (8 pages); listings of final observed and calculated structure factors for **4c** and **15b** (23 pages). Ordering information is given on any current masthead page.